RIVISTA DEL NUOVO CIMENTO VOL. 3, N. 11 1980

General-Relativistic Analysis of Charged-Particle Motion in Electromagnetic Fields Surrounding Black Holes.

A. R. PRASANNA

Physical Research Laboratory - Navrangpura, Ahmedabad 380009, *India*

(ricevuto il 23 Maggio 1980)

1. – Introduction and motivation.

Einstein's general theory of relativity considered as the most beautiful creation of a single mind is just not only a beautiful theory, but also has been vindicated as the most viable theory of astrophysics [1]. Though theoretical astrophysics has been a subject well pursued since the time of Jeans and Eddington, it got a tremendous impetus during the last two decades after the advances in radioastronomy. Thanks to the modern developments in space technology, today wa are able to study the Universe through the entire electromagnetic spectrum starting from radiowaves and going up to γ-rays. The last few years have seen the birth of infra-red astronomy, ultraviolet astronomy, X-ray astronomy and γ-ray astronomy. One of the fundamental contributions of general relativity to astrophysics is the gravitational-wave astronomy which is being pursued very seriously. Excellent review articles exist on the status of these fields as of today [2]. As a consequence of these developments we are now aware of a most astounding Universe around us consisting of very-high-energy reservoirs like quasars and X-ray binaries, on the one hand, and intriguing clocks like pulsars and perhaps the black holes, on the other. It is a kind of feast for theoretical astrophysicists to play around with theories and

construct models for these high-energy sources. But so far no convincing theory has been proposed to explain the radiation from these sources. Though the definite mechanism has not been understood, it is generally believed that the radiation emission could be due to plasma processes near compact objects like neutron stars and black holes [3]. Thus it becomes necessary to consider plasma processes in intense-gravitational-field backgrounds, as such compact objects would be massive enough to produce noticeable space-time curvature effects. There have been treatments wherein models do take into account gravitational fields, but restrict themselves to a Newtonian formulation. Surely these treatments are not adequate enough if one is thinking of black holes as the source of gravitational field. Few models do take into account special-relativistic effects up to the extent of considering the charged particles to have very high velocities [4]. In our opinion the discussions of plasma processes in such situations, particularly those concerning accretion plasma disks, should be taken up on a curved-background geometry, as even a $1M_{\odot}$ neutron star will have a very high gravitational field in its immediate vicinity and more so in the case of black holes. As a prelude to considering plasma processes on curved background (general-relativistic formulation), it is necessary to first consider single-particle dynamics, before going onto collective effects. This prompted us to review the state of the subject-particle orbit theory in general relativity, particularly concerning the characteristic trajectories of charged-particle motion in various background geometries with combined electromagnetic and gravitational fields.

In fact it is well known that the best way to understand the structure of any field is to study the dynamics of test particles in that field. In general relativity, wherein the gravitation is represented by the space-time curvature of the underlying manifold, the structure of the manifold can be completely studied through the geodesics of the manifold which represent the trajectories of test particles in the absence of any other external field [5]. Along with the gravitational field, if there are other fields present like a Coulomb field or a spin field, the particle trajectories will still be geodesics only if the gravitational field does not interact with these external fields. On the other hand, if the particle is charged or has spin, then the particle deviates from its geodesic motion and the study of such trajectories would reveal information about the influence of these interacting fields on the geometry and *vice versa*. Concerning the study of geodesics, there already exists a number of articles [6] and thus we restrict this review only to the motion of charged particles in combined gravitational and electromagnetic fields.

The trajectories of a charged particle of charge e and rest mass M_0 in an electromagnetic field in general relativity are given by the covariant Lorentz equations

$$u^i_{;j}u^j = (e/M_0)F^i{}_j u^j , \tag{1.1}$$

wherein $u^i = \mathrm{d}x^i/\mathrm{d}s$ is the four-velocity of the particle and $F^i{}_j$ is the electromagnetic-stress tensor. The semi-colon denotes the covariant derivative, taken with respect to the space-time metric associated with the background geometry as given by

$$\mathrm{d}s^2 = g_{ij}\mathrm{d}x^i\mathrm{d}x^j\,. \tag{1.2}$$

In general g_{ij}, the metric potentials, should be obtained as solutions of the combined set of Einstein-Maxwell equations in the usual notation

$$R_{ij} - \tfrac{1}{2}Rg_{ij} = -\,(8\pi G/c^2)\,E_{ij}\,, \tag{1.3}$$

wherein E_{ij}, the source term, is provided by the accompanying electromagnetic field

$$E_{ij} = F_{ik}F_j{}^k - \tfrac{1}{4}g_{ij}F_{kl}F^{kl} \tag{1.4}$$

with F_{ij} satisfying the covariant Maxwell equations

$$F^{ij}{}_{;j} = J^i\,, \qquad F_{ij,k} + F_{jk,i} + F_{ki,j} = 0\,, \tag{1.5}$$

J^i being the current vector.

Thus, in principle, to get the trajectories of charged particles in a manifold with space-time curvature produced by certain electromagnetic fields, given by F_{ij}, satisfying (1.5), one should solve (1.3) for g_{ij}, using these F_{ij} and then integrate the orbit equations (1.1), using the g_{ij} so obtained. This is well said in principle, whereas in practice it is almost impossible to solve exactly the complete set of Einstein-Maxwell equations for arbitrary electromagnetic fields. Recently KINNERSLEY and CHITRE [7] have extended an earlier prescription of Kinnersley for generating space-time metrics for stationary axially symmetric fields by using an infinite-parameter symmetry group of transformations, a review of which may be found in [8]. However, the solutions so obtained would not all be physically plausible, as all the transformations involved do not preserve asymptotic flatness. There are quite many solutions with cylindrically symmetric electromagnetic fields [9], but these again are not all astrophysically significant. Our aim in this review being a study of charged-particle motion in astrophysical situations, we will consider only solutions of astrophysical interest.

It is indeed remarkable that the only known class of solutions of astrophysical interest are the ones from the Kerr-Newman family [10] (which incidentally are exact solutions of the Einstein-Maxwell equations) which represent the geometry outside a black hole with three characteristics, the mass m, the charge Q

and the angular momentum a, given by the live element:

$$(1.6) \qquad ds^2 = -(\Delta/\Sigma)[dt - a\sin^2\theta\, d\varphi]^2 + (\Sigma/\Delta)\, dr^2 + \\ + \Sigma\, d\theta^2 + (\sin^2\theta/\Sigma)[(r^2 + a^2)\, d\varphi - a\, dt]^2,$$

wherein

$$\Delta = r^2 - 2mr + a^2 + Q^2, \qquad \Sigma = r^2 + a^2\cos^2\theta\,.$$

As is well known, this solution reduces to that of Kerr ($Q = 0$), Reissner-Nordström ($a = 0$) and Schwarzschild ($a = 0$, $Q = 0$). Because of the charge and rotation there is an induced magnetic-dipole field of moment Qa. CARTER was the first to obtain the complete set of integrals of motion for a charged particle in this geometry. He elegantly exploited the fact that the charged Klein-Gordon equation in this field is separable, which in turn ensured the separability of the Hamilton-Jacobi equation. A detailed review of this work may be found in [11]. RUFFINI and his co-workers [12] have worked out the dynamics of charged particles in the Kerr-Newman and Reissner-Nordström fields, whereas HOJMAN and HOJMAN [13] have discussed the motion of spinning charged particles in the Kerr-Newman background. However, in these classes of solutions the basic field associated with the central star is an electrostatic field due to the charge, apart from the gravitational field. But astrophysically more interesting are solutions having electromagnetic fields, as most of the celestial bodies are endowed with magnetic fields rather than net charges. Hence one should look for solutions of Einstein-Maxwell equations which are asymptotically flat and have nonzero dipole magnetic moment, even in the absence of rotation. These systems of equations are formidable to solve in general. However, there are some solutions obtained by perturbation techniques under the assumption that the electromagnetic field is weak compared to the gravitational field and thus it does not affect the basic geometry. This is achieved essentially by solving the curved-space Maxwell equations on a given background. This assumption is not bad, for even the most intense magnetic field associated with pulsars of, say, about 10^{12} G carries an energy which is very small compared to the gravitational potential energy on the surface of a neutron star of $1 M_\odot$. Thus it is quite reasonable to assume that the magnetic field would not affect the space-time curvature, but the curvature could affect the magnetic field. With such an assumption GINZBURG and OZERNOI [14], PETTERSON [15] and more recently BICAK and DVORAK [16] have obtained solutions for a dipole magnetic field on Schwarzschild background, whereas using a similar approach CHITRE and VISHVESHWARA [17], PETTERSON [18] and KING *et al.* [19] have obtained solutions for stationary electromagnetic fields on a Kerr background. WALD [20] has obtained a solution for a uniform magnetic field on a Kerr background. Charged-particle dynamics in such electro-

magnetic fields have been extensively studied by PRASANNA and VARMA [21] for the Schwarzschild background and by PRASANNA and VISHVESHWARA [22] and PRASANNA and CHAKRABORTY [23] for the Kerr background.

We give in sect. **2** the basic approach in all these studies which is almost the same (Lagrangian formulation) and in sect. **3** we consider the trajectories in Reissner-Nordström and Kerr-Newmann geometries. In sect. **4** we consider the trajectories of a spinning charged particle and in sect. **5** particle dynamics in electromagnetic fields superposed on Schwarzschild and Kerr background geometries. Section **6** deals with motion in Ernst space-time and sect. **7** gives some discussions.

The notation adopted is more or less usual with Einstein's summation convention and the differentiation with respect to the path parameter s being indicated by an overhead dot. The physical parameters that appear are normalized with respect to the particle rest mass M_0 and we use throughout spherical polar co-ordinates r, θ, φ alongwith the natural units $G = 1$, $c = 1$ and the signature of the metric $+2$.

2. – Basic approach.

In all the cases that we are going to consider the gravitational as well as the electromagnetic fields are both axisymmetric or spherically symmetric and stationary or static. These symmetries imply the existence of two Killing vectors, ξ^i the timelike Killing vector, corresponding to the total energy of the particle being a constant of motion and ζ^i the spacelike one, corresponding to the canonical angular momentum of the particle being a constant of motion.

In the absence of interacting external fields the scalars $\xi^i u_i = -E$ and $\zeta^i u_i = l$ are constants along the geodesics:

$$u^i_{;j} u^j = 0 . \tag{2.1}$$

On the other hand, in the presence of external electromagnetic fields, these scalars are generalized in a simple way as given by

$$(u_i + eA_i)\,\xi^i = -E \tag{2.2}$$

and

$$(u_i + eA_i)\,\zeta^i = l , \tag{2.3}$$

which are constants along the trajectories

$$u^i_{;j} u^j = eF^i{}_j u^j , \tag{2.4}$$

if and only if the vector potential A_i satisfies the Lie transport equation

$$A_{i;j}K^j + A_j K^j_{;i} = 0\,, \tag{2.5}$$

wherein K^i is any Killing vector and

$$F_{ij} = A_{j,i} - A_{i,j}\,. \tag{2.6}$$

In the above treatment, the Killing vectors ξ^i and ζ^i are normalized and are given by

$$\xi^i = \delta^i{}_t\,, \qquad \zeta^i = \delta^i{}_\varphi\,. \tag{2.7}$$

These features may also be clearly brought out in a Lagrangian formalism (which is generally used) as follows. For a particle of rest mass M_0 and charge e moving in combined gravitational and electromagnetic fields represented by the potentials g_{ij} and A_i, respectively, the Lagrangian of motion is given by

$$\mathscr{L} = \tfrac{1}{2} g_{ij}\dot{x}^i\dot{x}^j + eA_i\dot{x}^i\,. \tag{2.8}$$

If the fields are stationary (or static) and axisymmetric (or spherically symmetric), then the Lagrangian is independent of the time co-ordinate t and the azimuthal co-ordinate φ. This naturally gives two constants of motion:

$$\partial\mathscr{L}/\partial\dot{t} = -E \tag{2.9}$$

and

$$\partial\mathscr{L}/\partial\dot{\varphi} = l\,. \tag{2.10}$$

By identifying the four-vector u^i as $\mathrm{d}x^i/\mathrm{d}s$, it may be easily seen that (2.9) and (2.10) are the same as (2.2) and (2.3), as the most general class of metric that we intend to use in our discussion is stationary and axisymmetric, *viz.*

$$\mathrm{d}s^2 = g_{rr}\,\mathrm{d}r^2 + g_{\theta\theta}\,\mathrm{d}\theta^2 + g_{\varphi\varphi}\,\mathrm{d}\varphi^2 + 2g_{t\varphi}\,\mathrm{d}t\,\mathrm{d}\varphi + g_{tt}\,\mathrm{d}t^2 \tag{2.11}$$

with g_{ij} being functions of r and θ alone.

The above two constants of motion may be written as

$$g_{tt}u^t + g_{t\varphi}u^\varphi = -(E + eA_t) \tag{2.12}$$

and

$$g_{\varphi t}u^t + g_{\varphi\varphi}u^\varphi = l - eA_\varphi\,. \tag{2.13}$$

From these two equations we can straightaway obtain two first integrals of motion u^t and u^φ as given by

$$u^t = \frac{-[g_{\varphi\varphi}(E + eA_t) + g_{t\varphi}(l - eA_\varphi)]}{g_{\varphi\varphi}g_{tt} - g_{t\varphi}^2}, \tag{2.14}$$

$$u^\varphi = \frac{g_{t\varphi}(E + eA_t) + g_{tt}(l - eA_\varphi)}{g_{\varphi\varphi}g_{tt} - g_{t\varphi}^2}. \tag{2.15}$$

As we will be interested only in considering trajectories of real particles (tardyons) the velocity four-vector u^i should be timelike, which for metric of signature $+2$ is expressed as

$$g_{ij}u^i u^j = -1, \tag{2.16}$$

which gives us one more first integral of motion. If in particular one considers the trajectories in the equatorial plane of the central source given by $\theta = \pi/2$, $u^\theta = 0$, then eqs. (2.14) to (2.16) will give all the information about the nature of the orbits. In this case u^r, the other first integral, may be obtained directly by using u^t and u^φ from (2.14), (2.15) in (2.16) as

$$(u^r)^2 = \frac{-1}{g_{rr}D} \cdot \{D + g_{tt}(l - eA_\varphi)^2 + g_{\varphi\varphi}(E + eA_t)^2 + 2g_{t\varphi}(E + eA_t)(l - eA_\varphi)\}, \tag{2.17}$$

wherein

$$D = g_{\varphi\varphi}g_{tt} - g_{t\varphi}^2 .$$

As u^r gives the particle proper velocity in the r-direction if one considers the equation $u^r = 0$, it gives the turning points for the particle in its orbit. Further, at the points $u^r = 0$ the particle is in equilibrium under the interacting gravitational, electromagnetic and centrifugal forces and thus the energy of the particle $E_{\min}$, calculated at $u^r = 0$, gives the «effective potential energy» that it carries when subject to the balancing forces. Thus, by solving the equation $u^r = 0$ for E, one can compute the «effective potential», often denoted by V_{eff}, for the particle in its r-motion. Then, by studying the structure of V_{eff}, for different values of the constants l and E, one can get a complete picture of the nature of orbits regarding their boundedness and stability. This approach of analysing the particle orbits is well known and has been used earlier by many authors in connection with the study of geodesics [6].

From (2.17), by taking $u^r = 0$, the effective potential may be obtained as given by

$$V_{\text{eff}} \equiv E_\pm = -eA_t - (g_{t\varphi}/g_{\varphi\varphi})(l - eA_\varphi) \pm (1/g_{\varphi\varphi})\{-D[g_{\varphi\varphi} + (l - eA_\varphi)^2]\}^{\frac{1}{2}}, \tag{2.18}$$

the $\pm$ indicating the positive- and negative-energy states for the particle, with obviously different domains of dependence.

3. – Motion in Reissner-Nordström and Kerr-Newman geometries.

As mentioned in the introduction, the Kerr-Newman solution which includes the Reissner-Nordström one has now been fully established as the unique solution of the Einstein-Maxwell equations representing the external field of a black hole with mass, charge and angular momentum. The study of the charged-particle motion in these geometries has been considered by many authors and we presently discuss the results of Ruffini and co-workers [24-26] for the RN geometry and of Hojman and Hojman [13] for a charged spinning particle in the KN geometry.

The Reissner-Nordström metric

$$(3.1) \qquad ds^2 = -(1 - 2m/r + Q^2/r^2)\,dt^2 + (1 - 2m/r + Q^2/r^2)^{-1}dr^2 + \\ + r^2\,d\theta^2 + r^2\sin^2\theta\,d\varphi^2$$

represents the space-time exterior to a self-gravitating charged mass, with charge Q and mass m (both expressed in length units), whose electrostatic field is given by the vector potential

$$(3.2) \qquad A_i = (0, 0, 0, -Q/r)\,.$$

If one considers a charged particle in this space-time, with charge e and mass M, then in the equatorial plane of the central body one can obtain the effective potential for the r-motion of the particle from (2.18) as given by

$$(3.3) \qquad V_{\text{eff}} = \frac{eQ}{r} \pm \left[\left(1 - \frac{2m}{r} + \frac{Q^2}{r^2}\right)\left(1 + \frac{l^2}{r^2}\right)\right]^{\frac{1}{2}}.$$

As mentioned earlier, the $\pm$ sign corresponds, respectively, to the positive- and negative-root states $E_\pm$, such that

$$(3.4) \qquad \lim_{r\to\infty} E_+ = +M_0 \qquad \text{and} \qquad \lim_{r\to\infty} E_- = -M_0\,.$$

Figure 1 gives the effective-potential curves as obtained by Ruffini for different values of e, for a fixed l in the case of the extreme Reissner-Nordström solution for $Q = m$. Depending on the charge e, one would have $eQ > 0$ or < 0, wherein for the case $eQ < 0$ negative-energy states of positive-root so-

lution can exist in the region

$$m + (m^2 - Q^2)^{\frac{1}{2}} \leqslant r \leqslant m + [m^2 - Q^2(1 - e^2)]^{\frac{1}{2}}, \tag{3.5}$$

called the « effective ergosphere ».

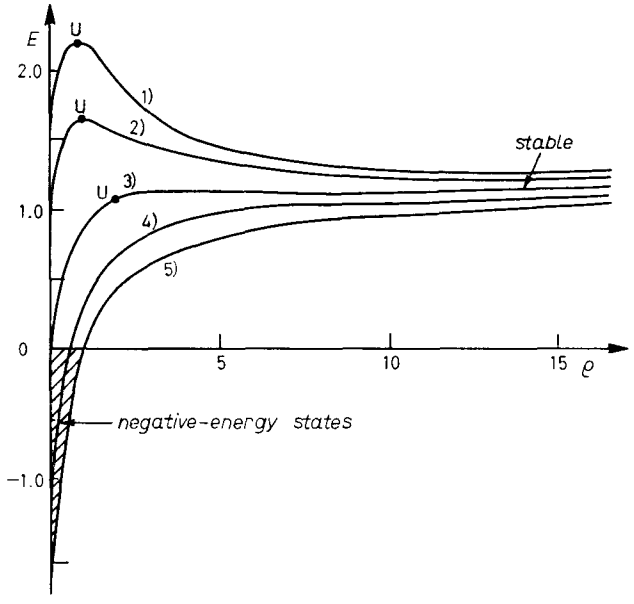

Fig. 1. – Effective potential V_{eff} in an extreme Reissner-Nordström geometry ($Q/m = 1$) for a particle of charge e and rest mass M_0 [12]: 1) $e/M_0 = 2.0$, 2) $e/M_0 = 1.0$, 3) $e/M_0 = 0.0$, 4) $e/M_0 = -1.0$, 5) $E/M_0 = -2.0$, U = unstable.

DENARDO and RUFFINI [24] conclude that, as a consequence of such solutions, it would be possible to extract electrostatic energy from a Reissner-Nordström black hole in the same sense as in Penrose process for Kerr black holes, which is envisaged as follows: a particle P_0 coming from infinity enters the effective ergosphere, wherein it splits (decays) into two particles P_1 and P_2 such that the particle P_1 with a charge opposite to that of the black hole is suitably projected inside the horizon, whereas P_2 is pushed out with energy higher than that of P_0, the incident particle. It has been claimed [12] that, if an extreme Reissner-Nordström solution is transformed into a Schwarzschild solution by reversible transformations, up to 50% of the total energy of the black hole can be extracted. However, in our opinion, this process of energy extraction is extremely unnatural for two reasons: i) it is highly improbable that black holes with net charge (like the RN black hole) will stay in equilibrium at sites where continuous pair production could be taking place, and

ii) as there are no magnetic fields associated with such black holes, the particle decay mechanism cannot be very effective.

From the effective-potential curves (fig. 1) it can be seen that the charged particle can have circular orbits corresponding to the extrema of V_{eff}, of which some are stable and others unstable. RUFFINI and ZERILLI [26] have analysed these circular orbits, the equations governing which are given by

$$(u^t)_0 = \left\{\frac{eQ}{2r_0} + \left(1 - \frac{3m}{r_0} + \frac{2Q^2}{r_0^2} + \frac{Q^2e^2}{4r_0^2}\right)^{\frac{1}{2}}\right\}^{-1}, \tag{3.6}$$

$$\omega_0^2 = \left(\frac{m}{r_0^3} - \frac{Q^2}{r_0^4}\right) - \frac{eQ}{r_0^3}\Big/(u^t)_0, \tag{3.7}$$

$$E = \frac{eQ}{r_0} + \left(1 - \frac{2m}{r_0} + \frac{Q^2}{r_0^2}\right)(u^t)_0. \tag{3.8}$$

Wherein r_0 denotes the radius of the orbit and $\omega_0 = (\mathrm{d}\varphi/\mathrm{d}t)_{r_0}$ the angular velocity measured by a distant observer. These equations may be obtained directly from the general equations of sect. **2** for the metric (3.1) through the conditions defining a circular orbit given by

$$(u^r)_{r=r_0} = 0, \qquad (\mathrm{d}u^r/\mathrm{d}r)_{r=r_0} = 0, \tag{3.9}$$

which give, respectively,

$$\left(1 - \frac{2M}{r_0} + \frac{Q^2}{r_0^2}\right)(u^t)_0^2 = 1 + r_0^2\omega_0^2(u^t)_0^2 \tag{3.10}$$

and

$$\left(\frac{M}{r_0^2} - \frac{Q^2}{r_0^3}\right)(u^t)_0^2 = \frac{eQ}{r_0^2}(u^t)_0 + r_0\,\omega_0^2(u^t)_0^2. \tag{3.11}$$

As has been found by RUFFINI and ZERILLI, these circular orbits are stable if and only if $eQ/m < 1$. The radius and the binding energy of the tightly bound circular orbit increases with the value of $|eQ|$. In the limit $|eQ| \to \infty$, they find the energy of the particle to go as

$$E \approx -2[(r_0 m - Q^2)/(r_0^2 - 3mr_0 + 2Q^2)](eQ/r_0) - \\ - (r_0^2 - 2mr_0 + Q^2)/eQr_0 + \theta(r_0/eQ)^3, \tag{3.12}$$

whereas for the maximum bound orbit the radius and the energy are given by

$$r_{\max} \approx (\sqrt{2}\,|eQ|)^{\frac{2}{3}} \tag{3.13}$$

and

$$E_{\max} \approx \frac{3m}{2}(2/|eQ|)^{\frac{1}{2}}, \tag{3.14}$$

which in fact corresponds to the last stable circular orbit. On the other hand, the structure of the effective potential shows that it is possible to have few more circular orbits which are but unstable. Of these orbits the last one occurs for $E \to \infty$ and thus found to be at

$$r = r_{\min} = [3m + (9m^2 - 8Q^2)^{\frac{1}{2}}]/2\,. \tag{3.15}$$

In fact it is interesting to see that this last unstable circular orbit occurs at the same value of r even in the case of an uncharged particle [27].

Thus a charged particle in the vicinity of a Reissner-Nordström black hole can have circular orbits which are unstable in the region

$$r_{\min} < r < r_{\max}$$

and stable for $r > r_{\max}$. In general the parameters of the last stable circular orbit can be obtained from the expression for the effective potential by using the criteria of stability through the extrema of the effective potential. RUFFINI and ZERILLI point out that the binding energy of a particle in the last stable orbit increases very rapidly with decreasing value of e and the particle velocity, say V_p, tends towards the local light velocity V_c, whereas in the entire family of unstable circular orbits for a fixed value of e the ratio V_p/V_c increases monotonically for discreasing values of the radius and $V_p \to V_c$ as the radius $\to r_{\min}$.

While analysing these orbits, RUFFINI and co-workers have also considered the question of radiation emission and this we shall consider at a later stage.

As pointed out earlier, CARTER has given a very general treatment for the dynamics of a charged particle in the vicinity of a Kerr-Newman black hole, wherein he has obtained the complete set of first integrals of the orbit equation as

$$\begin{cases} \Sigma u^r = R^{\frac{1}{2}}, \qquad \Sigma U^\theta = \Theta^{\frac{1}{2}}, \\ \Sigma u^t = -\,a(aE\sin^2\theta - l) + (r^2 + a^2)\,P\Delta^{-1}, \\ \Sigma u^\varphi = -\,(aE - l/\sin^2\theta) + aP\Delta^{-1}, \end{cases} \tag{3.16}$$

wherein

$$\begin{cases} P = E(r^2 + a^2) - la - eQr, \\ R = P^2 - \Delta(r^2 + K), \\ \Theta = K - \cos^2\theta[a^2(1 - E^2) + l^2/\sin^2\theta] - (l - aE)^2, \end{cases} \tag{3.17}$$

K, E and l being constants of the motion along the trajectory of the particle and Σ and Δ, the metric coefficients as defined in (1.6). The effective potentials for the r-motion and θ-motion may be obtained directly by solving $R = 0$ and $\Theta = 0$, respectively. Some qualitative remarks concerning circular orbits may be found in [28].

4. – Motion of a charged spinning particle.

Apart from the charge, if the particle also possesses spin, then there will be dynamical effects because of either spin-orbit coupling or spin-spin coupling. In the case of a spinning particle again the particle orbit will not be geodesic. Though the general equations of motion of a spinning test particle were first obtained by MATHISON [29], the equations are known after PAPAPETROU, who derived them for the general pole-dipole particles [30], and are given by

$$\frac{DP^\mu}{Ds} = -\frac{1}{2} R^\mu{}_{\nu\alpha\beta} u^\nu S^{\alpha\beta} \tag{4.1}$$

and

$$\frac{DS^{\mu\nu}}{Ds} = S^{\mu\lambda} \sigma_\lambda{}^\nu - \sigma^{\mu\lambda} S_\lambda{}^\nu , \tag{4.2}$$

wherein P^μ and $S^{\alpha\beta}$ are the canonical linear and angular momentum of the particle connected through the relation

$$P^\mu u^\nu - P^\nu u^\mu = S^{\mu\lambda} \sigma_\lambda{}^\nu - \sigma^{\mu\lambda} S_\lambda{}^\nu \tag{4.3}$$

with u^μ and $\sigma^{\mu\lambda}$ representing the particle four-velocity and the angular velocity. D/Ds as usual represents the covariant derivative and $R^\mu{}_{\nu\alpha\beta}$ represents the space-time curvature tensor of the underlying manifold.

PRASANNA and KUMAR [31] have considered the motion of a spinning charged particle as governed by eqs. (4.1) and (4.2) in an axial magnetic field as given by Melvin's magnetic universe [32]

$$ds^2 = \exp[2\psi](dt^2 - dr^2 - dz^2) - r^2 \exp[-2\psi] d\varphi^2 \tag{4.4}$$

with $\psi = \ln(1 + \pi B^2 r^2)$, B being the magnetic-field intensity. In the approximation wherein they neglected the spin-orbit coupling they found that the particle in a circular orbit will not be disturbed very much and that the spin precession is affected very little by the gravitational field due to the magnetic energy. On the other hand, their equations indicate that, if the spin-orbit coupling is not neglected, then the particle seems to execute an oscillatory

motion along the Z-axis, which perhaps will show some distinctive polarization of the emitted characteristic radiation.

It is natural to expect more interesting result if, instead of background geometry like Melvin universe, one has the field of a black hole. This aspect has been fully discussed by HOJMAN and HOJMAN, who have considered the motion of a spinning charged particle in the Kerr-Newman geometry.

Unlike in the case of a spinless particle, in the case of a spinning particle the first thing to notice is that the particle momentum π^μ is not necessarily parallel to its four-velocity u^μ. As proved by HANSON and REGGE for the case of pure gravitational field and by HOJMAN and HOJMAN for the case of gravitational and electromagnetic fields, these two quantities are related through the equation

$$u^\mu = \pi_\alpha u^\alpha \left\{ \pi^\mu + \frac{S^{\mu\lambda} f_{\lambda\varrho} \pi^\varrho}{1 + \frac{1}{2} S^{\alpha\beta} f_{\alpha\beta}} \right\}, \tag{4.5}$$

wherein

$$f_{\alpha\beta} = -\tfrac{1}{2} R_{\alpha\beta\mu\nu} S^{\mu\nu} - eF_{\alpha\beta} \tag{4.6}$$

and

$$g_{\mu\nu}\pi^\mu\pi^\nu = -1\,, \tag{4.7}$$

$$S^{\mu\nu}S_{\mu\nu} = 2J^2\,. \tag{4.8}$$

With this the generalized momentum P^μ is given by

$$P^\mu = \pi^\mu - eA^\mu\,, \tag{4.9}$$

A^μ being the electromagnetic vector potential, and the Papapetrou equations now read

$$\frac{\mathrm{D}\pi^\mu}{\mathrm{D}s} = -\frac{1}{2} R^\mu{}_{\nu\alpha\beta} u^\nu S^{\alpha\beta} - eF^\mu{}_\nu u^\nu \tag{4.10}$$

and

$$\frac{\mathrm{D}S^{\mu\nu}}{\mathrm{D}s} = S^{\mu\lambda}\sigma_\lambda{}^\nu - \sigma^{\mu\lambda}S_\lambda{}^\nu \equiv \pi^\mu u^\nu - \pi^\nu u^\mu\,. \tag{4.11}$$

These equations are generally solved with the supplementary condition

$$S^{\mu\nu}\pi_\nu = 0\,. \tag{4.12}$$

The Kerr-Newman geometry as given in (1.6) has an electromagnetic field given by

$$\begin{cases} F_{tr} = Q\Sigma^{-2}(r^2 - a^2\cos^2\theta)\,, \\ F_{t\theta} = -2Q\Sigma^{-2}a^2 r\sin\theta\cos\theta\,, \\ F_{r\varphi} = Q\Sigma^{-2}a\sin^2\theta(r^2 - a^2\cos^2\theta)\,, \\ F_{\theta\varphi} = -2Q\Sigma^{-2}ar(r^2 + a^2)\sin\theta\cos\theta\,. \end{cases} \tag{4.13}$$

As the fields are stationary and axisymmetric, the two constants of motion E and l are given by

$$\pi_t - \tfrac{1}{2} g_{t\mu,\nu} S^{\mu\nu} + [eQr/(r^2 + a^2\cos^2\theta)] = -E\,, \tag{4.14}$$

$$\pi_\varphi - \tfrac{1}{2} g_{\varphi\mu,\nu} S^{\mu\nu} - [eQar\sin^2\theta/(r^2 + a^2\cos^2\theta)] = l\,. \tag{4.15}$$

As the general motion of the spinning charged particle in this background is too complicated, HOJMAN and HOJMAN consider as usual the motion in the equatorial plane with the further assumption that the spin of the particle is orthogonal to this plane, after establishing that this motion exists. The effective potential for the r-motion in the equatorial plane is given by

$$V_{\text{eff}} \equiv E_\pm = [\beta \pm (\beta^2 - \alpha r)^{\frac{1}{2}}]/\alpha\,, \tag{4.16}$$

wherein $\pm$ stand for the same notation as in (2.18) and

$$\alpha = -k_1\,, \qquad \beta = -ek_1 Q/r + (l - eaQ/r)k_3 \tag{4.17}$$

$$\begin{cases} r = -\dfrac{e^2Q^2}{r^2}k_1 + \dfrac{2eQ}{r}\left(l - \dfrac{eaQ}{r}\right)k_3 - \left(l - \dfrac{eaQ}{r}\right)^2 k_2 + \delta^2\Delta\,, \\ k_i = A_i J^2/r^2 + B_i J/r + C_i\,, \end{cases} \tag{4.18}$$

A_i, B_i, C_i being given by

$$\begin{cases} A_1 = \dfrac{1}{r^4}[r^2(r^4 - 2mr^3 - 2ma^2 r - m^2a^2) + \\ \qquad\qquad + Q^2(r^4 + 2a^2r^2 + 2ma^2 r - Q^2a^2)]\,, \\ A_2 = -\dfrac{1}{r^4}[m^2r^2 + Q^2(Q^2 - 2mr)]\,, \\ A_3 = \dfrac{a}{r^4}[mr^2(m + r) - Q^2(r^2 + 2mr - Q^2)]\,, \\ B_1 = \dfrac{2a}{r^3}[mr(3r^2 + a^2) - Q^2(2r^2 + a^2)]\,, \\ B_2 = \dfrac{2a}{r^3}(mr - Q^2)\,, \\ B_3 = \dfrac{1}{r^3}[r(r^3 - 3mr^2 - 2ma^2) + 2Q^2(r^2 + a^2)]\,, \\ C_1 = -\dfrac{1}{r^2}[r(r^3 + a^2r + 2ma^2) - Q^2a^2]\,, \\ C_2 = \dfrac{1}{r^2}[r(r - 2m) + Q^2]\,, \\ C_3 = \dfrac{a}{r^2}[2mr - Q^2]\,, \\ \delta^2 = [1 - (J^2/m^2r^4)(mr - Q^2)]^2\,, \end{cases} \tag{4.19}$$

J being the scalar associated with the total angular momentum (4.8). HOJMAN and HOJMAN particularly consider circular orbits with 100 % binding in the horizon of a maximal Kerr-Newman background ($a^2 + Q^2 = 1$). As the horizon in the equatorial plane for such a background is given by $r = m$, the conditions for such orbits are

$$(E)_{r=m} = 0\,, \qquad \left(\frac{\mathrm{d}E}{\mathrm{d}r}\right)_{r=m} = 0\,, \tag{4.20}$$

which give, respectively,

$$la + e(1 - a^2)^{\frac{1}{2}} = 0\,, \qquad (aJ - 1) \neq 0 \tag{4.21}$$

and

$$e^2(1 - a^2) = \frac{a^2(a^2J^2 - 1)^2}{[(1 + a - a^2)J + 1 + a][(1 - a - a^2)J - 1 + a]} \tag{4.22}$$

for $a \neq 0$.

As a^2 is never greater than 1, the denominator on the right-hand side can never be negative except perhaps when $a^2J^2 = 1$. This condition would give a strong restriction on the values of a and J that give rise to 100 % bound circular orbits. In the case of a spinless particle ($J = 0$) the criterion obtained here is the same as that of [25] for $a \to 1$ and $e^2(1 - a^2) \to \infty$. Figure 2 represents the curves $(1 + a - a^2)J + 1 + a = 0$, $(1 - a - a^2)J - 1 + a = 0$, $aJ + 1 = 0$, which imply $e \to \infty$ and $e \to 0$, respectively. In this figure the only points known earlier for 100 % binding orbits were those with $a = 1$ and $J = 0$ (CHRISTODOULOU

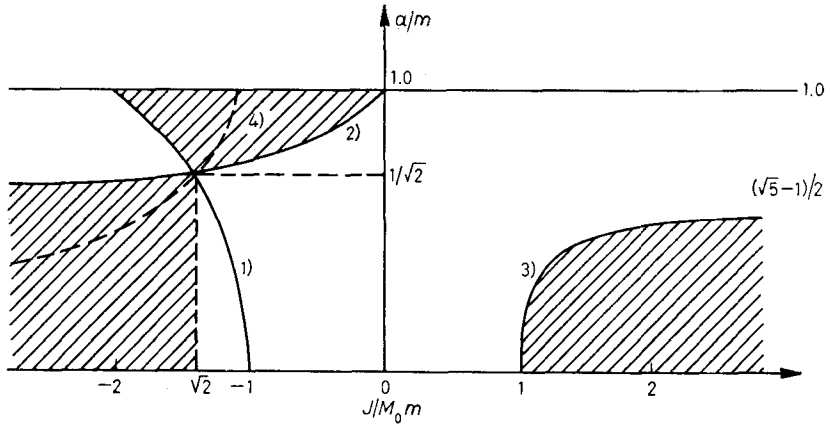

Fig. 2. – The curves $(1+a-a^2)J+1+a=0$ (1)), g (2)), $(1-a-a^2)J-1+a+0$ (3)) and $aJ + 1 = 0$ (4)). The hatched regions represent the points that give rise to real solutions for the charge e in eq. (4.22). Boundaries correspond to the limit $e \to \infty$. The curve $aJ + 1 = 0$, represented by the dashed line, is the locus of $e = 0$. The point $J = -\sqrt{2}$, $a = 1/\sqrt{2}$, where the three curves cross, is such that any e will satisfy eq. (4.22). The points $J = 0$, $a = 1$ and $J = -1$, $a = 1$ were obtained earlier in ref. [25, 33] ([13]).

and RUFFINI) and $J = -1$, $l = 0$ [33]. However, in this treatment, as the radius of the particle has an implicit restriction $R \geqslant J$, it is safer to consider the region $J/m \ll 1$ as physically relevant as only then the spin will be small and thus the radius also small characterizing a test particle. This restriction makes their allowed region for 100% binding to lie close to $Q = 0$, and thus in spite of their detailed treatment physically the results seem to be similar to that of Christodoulou and Ruffini and Tod *et al.* On the other hand, their treatment gains superiority over others for the reason that it shows the possibility of the particle acquiring superluminal velocity (u^μ can become space-like) for sufficiently large fields (gravitational and electromagnetic), a fact which needs to be examined closely after including higher multipoles and radiation in the analysis.

5. – Motion in stationary electromagnetic fields on a curved background.

As pointed out in the introduction, astrophysically more interesting discussions are the ones wherein charged-particle dynamics is considered in an electromagnetic field superposed on curved-background geometry. As seen in the previous sections, the Kerr-Newman solution represents electromagnetic fields of black holes with charge. But in Nature we are more likely to encounter situations wherein uncharged black holes could be immersed in external magnetic fields like the galactic magnetic field or have ring currents around them which would produce electromagnetic fields. Such situations are not covered by the Kerr-Newman family of solutions. In fact the electromagnetic fields in such situations would be quite small compared with the gravitational field associated with the black hole and thus would not disturb the background geometry of the space-time. On the other hand, the space-time curvature affects the electromagnetic fields and thus to describe such fields one has to solve Maxwell's equations on the given background manifold. Such solutions, as mentioned in the introduction, have been obtained by many authors [14-20] by using perturbation techniques. We will presently consider in detail charged-particle trajectories in these fields as obtained by PRASANNA and co-workers [21-23] for the Schwarzschild and Kerr background.

In order to obtain the structure of the electromagnetic field which is dipolar at infinity, superposed on the Schwarzshild geometry, GINZBURG and OZERNOI solve the Maxwell equations (1.5) on the background manifold:

$$(5.1) \qquad ds^2 = -\left(1-\frac{2m}{r}\right)dt^2 + \left(1-\frac{2m}{r}\right)^{-1} dr^2 + r^2\,d\theta^2 + r^2\sin^2\theta\,d\varphi^2\,,$$

by assuming the local Lorentz components of the field to be of the form

$$(5.2) \qquad F_{(\theta\varphi)} = 2\mu\frac{\cos\theta}{r^3}f(r)\,, \qquad F_{(\varphi r)} = \mu\frac{\sin\theta}{r^3}g(r)\,,$$

others being zero. Here μ is the magnetic-dipole moment and $f(r)$ and $g(r)$ are arbitrary functions to be determined. Maxwell's equations (1.5) with J^i, the current vector zero, give the two equations

$$\begin{cases} (\mathrm{d}/\mathrm{d}r)(f/r) + (g/r^2)(1 - 2m/r)^{-\frac{1}{2}} = 0\,, \\ (\mathrm{d}/\mathrm{d}r)[(g/r^2)(1 - 2m/r)^{\frac{1}{2}}] + 2f/r^3 = 0\,. \end{cases} \tag{5.3}$$

Solving for f and g, one can then get the two components $F_{(r\varphi)}$ and $F_{(\theta\varphi)}$ from which the components in the Schwarzschild frame may be obtained by using the relation

$$F_{kl} = \lambda^{(i)}{}_k \lambda^{(j)}{}_l F_{(ij)}\,, \tag{5.4}$$

$\lambda^{(i)}{}_k$ being the orthonormal tetrad associated with the Schwarzschild manifold. Once we have obtained F_{ij}, it is a matter of simple integration to get the vector potential A_i through relation (2.6) and in the present case A_i turns out to be

$$A_i = (0, 0, A_\varphi, 0)$$

with

$$A_\varphi = -\,(3\mu \sin^2\theta/8m^3)[r^2 \ln(1 - 2m/r) + 2m(r + m)]\,. \tag{5.5}$$

PRASANNA and VARMA have used this solution for determining the orbits of charged particles in a dipole magnetic field on the Schwarzschild manifold. The Lagrangian for the motion (2.8) is given by

$$\mathscr{L} = \frac{1}{2}\left\{-\left(1-\frac{2m}{r}\right)\dot{t}^2 + \left(1-\frac{2m}{r}\right)^{-1}\dot{r}^2 + r^2\dot{\theta}^2 + r^2\sin^2\theta\,\dot{\varphi}^2 - \right. \tag{5.6}$$
$$\left. - \frac{3e\mu\sin^2\theta}{4m^3}\left[r^2\ln\left(1-\frac{2m}{r}\right) + 2m(r+m)\right]\dot{\varphi}\right\}.$$

The two constants of motion E and l are found to be

$$\left(1-\frac{2m}{r}\right)\frac{\mathrm{d}t}{\mathrm{d}s} = E \tag{5.7}$$

and

$$r^2\sin^2\theta\,\frac{\mathrm{d}\varphi}{\mathrm{d}s} - \frac{3e\mu r^2\sin^2\theta}{8m^3}\left[\ln\left(1-\frac{2m}{r}\right) + \frac{2m}{r}\left(1+\frac{m}{r}\right)\right] = l\,, \tag{5.8}$$

whereas the equations governing the r and θ motion are given by

$$(5.9)\quad \frac{d^2r}{ds^2} - \frac{m}{r^2}\left(1-\frac{2m}{r}\right)^{-1}\left(\frac{dr}{ds}\right)^2 - r\left(1-\frac{2m}{r}\right)\left\{\left(\frac{d\theta}{ds}\right)^2 + \sin^2\theta\left(\frac{d\varphi}{ds}\right)^2\right\} + \\ + \frac{m}{r^2}\left(1-\frac{2m}{r}\right)\left(\frac{dt}{ds}\right)^2 = -\frac{3e\mu\sin^2\theta}{2m^3}\left[\left(1-\frac{m}{r}\right)+\left(\frac{r}{2m}-1\right)\ln\left(1-\frac{2m}{r}\right)\right]\frac{d\varphi}{ds},$$

$$(5.10)\quad \frac{d^2\theta}{ds^2} + \frac{2}{r}\frac{dr}{ds}\frac{d\theta}{ds} - \sin\theta\cos\theta\left(\frac{d\varphi}{ds}\right)^2 = \\ = -\frac{3e\mu\sin\theta\cos\theta}{4m^3}\left[\frac{2m}{r}\left(1+\frac{m}{r}\right)+\ln\left(1-\frac{2m}{r}\right)\right]\frac{d\varphi}{ds}.$$

Restricting the analysis to motion in the equatorial plane $\theta = \pi/2$, one can get the « effective potential » for the r-motion to be

$$(5.11)\quad V_{\text{eff}} = \left(1-\frac{2}{\varrho}\right)\left\{1+\varrho^2\left[\frac{L}{\varrho^2}+\frac{3\lambda}{8}\left\{\ln\left(1-\frac{2}{\varrho}\right)+\frac{2}{\varrho}\left(1+\frac{1}{\varrho}\right)\right\}\right]^2\right\},$$

wherein dimensionless parameters have been used such that $\varrho = r/m$ $L = l/m$, $\lambda = e\mu/m^2$, $\sigma = s/m$. By considering the limiting values of V_{eff}, one finds that, as $\varrho \to \infty$, $V_{\text{eff}} \to 1$, whereas, as $\varrho \to 2$, $V_{\text{eff}} \to 0$. It is interesting to see that in spite of the logarithmic singularity in the vector potential at $\varrho = 2$, which makes the magnetic-field components grow very large, the effective potential tends to zero as $\varrho \to 2$ because of the $1 - 2/\varrho$ term which dominates. This shows that at the event horizon the gravitational interaction (space-time curvature) dominates over all other interactions.

Figures 3-5 give some typical plots of the effective potential as a function of ϱ for different values of L and λ. The logarithmic singularity in the vector potential reflects through the appearance of an inner maximum E_{M_1} for V_{eff} very near $\varrho = 2$. Then the effective potential drops down to a sharp minimum still close to $\varrho = 2$ and then rises to a second maximum E_{M_2} which is the centrifugal barrier (it increases with increasing L). After this maximum V_{eff} again drops slowly towards the value 1. Very far from the source V_{eff} dips below 1, attains its flat minimum and then reaches 1 asymptotically. When $L < 0$, there is no centrifugal barrier and thus no potential well exists. Because of scaling difficulties, the plots do not show the inner maximum and the outer minimum. From the structure of the potential curves it may be seen that four different classes of orbits exist.

i) Highly relativistic particles with E^2 greater than both the maxima coming from infinity would find no barrier and thus plunge straight into the black hole.

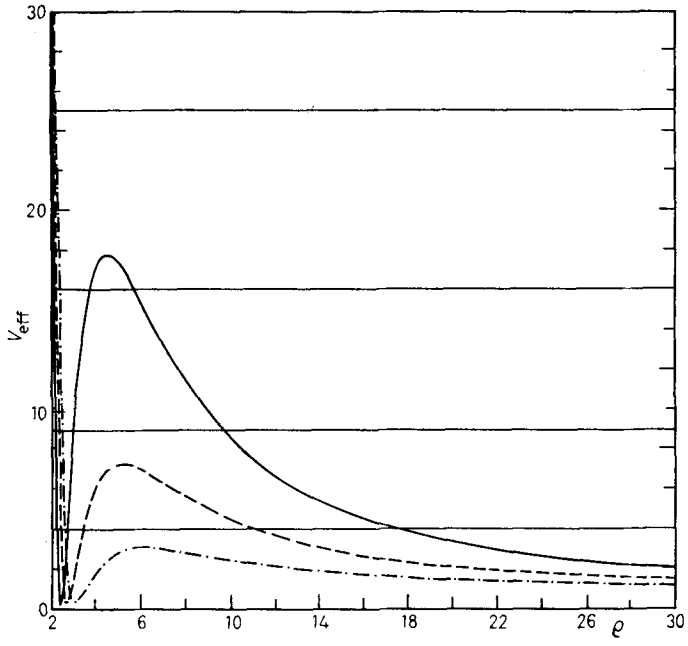

Fig. 3. – Plots of V_{eff} *vs.* $\varrho(=r/m)$ for different values of L, $\lambda = 27.5$: —·—·— $L = 17.6954$, – – – $L = 24.7736$, —— $L = 34.4136$. The inner maximum and the outer minimum are outside the limits of scaling. As λ increases the potential well flattens for a given L [21].

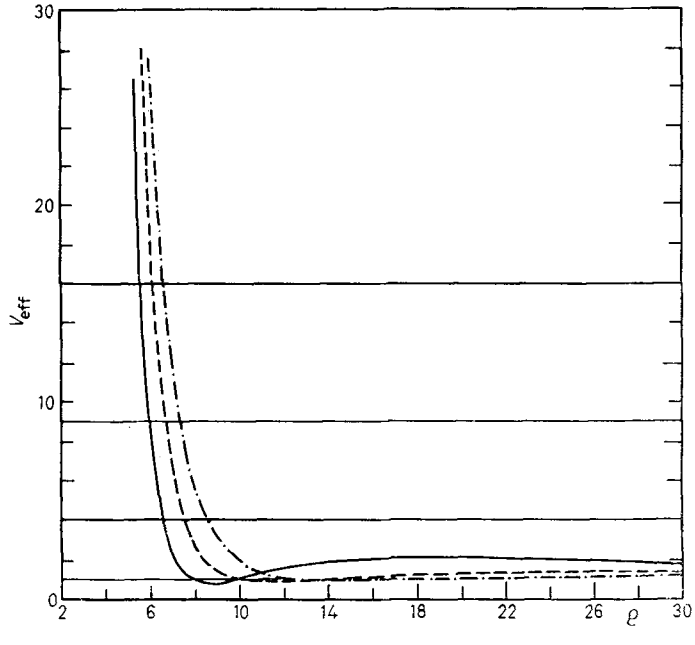

Fig. 4. – Same as fig. 3, but for $\lambda = 250$.

ii) If $E<E_{M_1}$, but greater than E_{M_2}, then the particle will have an unbound parabolic orbit. As it comes from infinity very near to the black hole, the magnetic field would turn it away and the particle will get back to infinity.

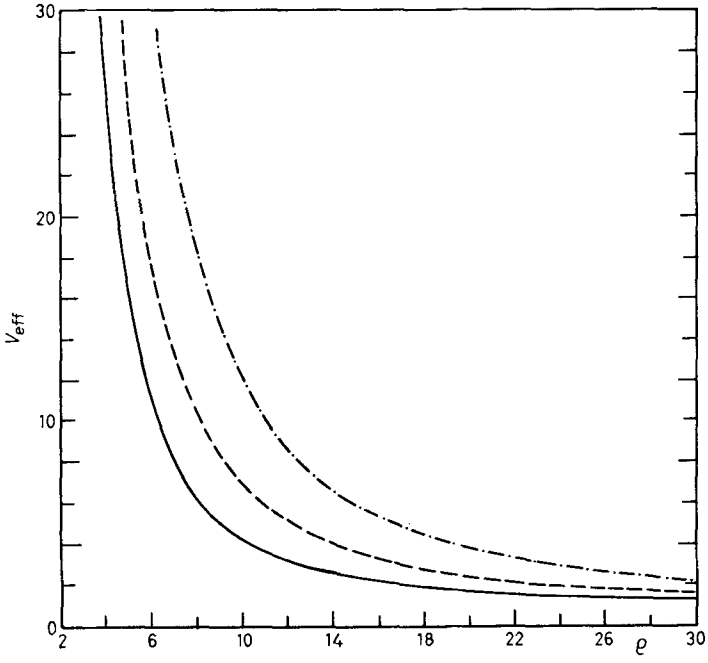

Fig. 5. – Same as fig. 3, but for $L=-34.4136$ (—·—·—), $L=-24.7736$ (— — —), $L=-17.6954$ (———).

iii) On the other hand, if its energy is such that $1<E<E_{M_2}$, then it will have four turning points, as may be seen from the curves. If the particle is coming from infinity, then it is unbound as the centrifugal barrier would turn it away. Instead, if the particle is inside the potential well, then it is bound in a stable orbit with the two turning points corresponding to the inner and outer envelope of the gyrating orbit. As this potential well is created by the magnetic field, the particle executes Larmor motion, as one is familiar with in the flat background. However, the important difference one finds is that unlike the case of flat background, wherein Larmor motion is circular (one talks of radius of gyration), here, as the magnetic field is modified by the space-time curvature (gravitational field), the Larmor circles are deformed into ellipses, as may be seen from the actual orbits (fig. 6-9). If either the seed magnetic field λ is large or the particle is sufficiently away from the event horizon (fig. 7, 8), gyration seems to be more circular than in the other two cases wherein the particle is closer to the event horizon and the magnetic field is weaker. These orbits are all stable as the particle is well inside the potential well and no perturbation will make them tunnel out.

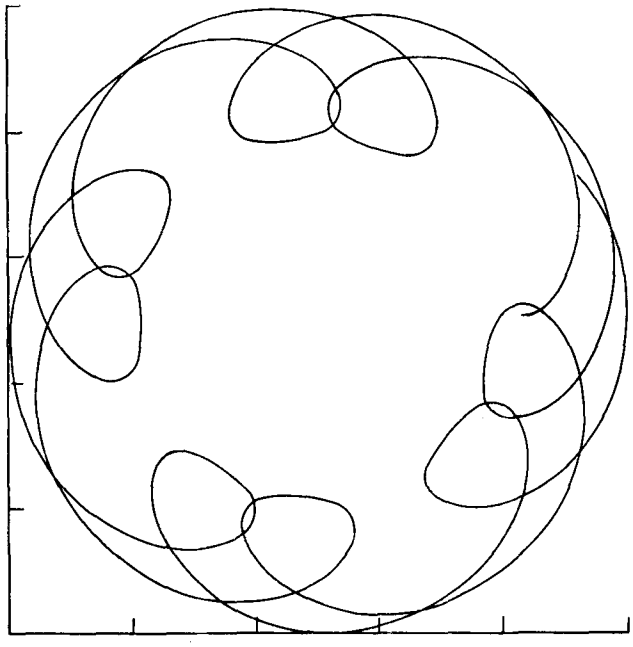

Fig. 6. – Equatorial-plane view of the orbits of a positively charged particle in a dipole magnetic field on the Schwarzschild background. The physical parameters are $E = 2$, $\lambda = 30$, $\varrho_0 = 3$, $L = 21.2345$. The turning points which correspond to the envelopes of gyrating orbits are $\varrho_1 = 2.562$, $\varrho_2 = 4.560$ [21].

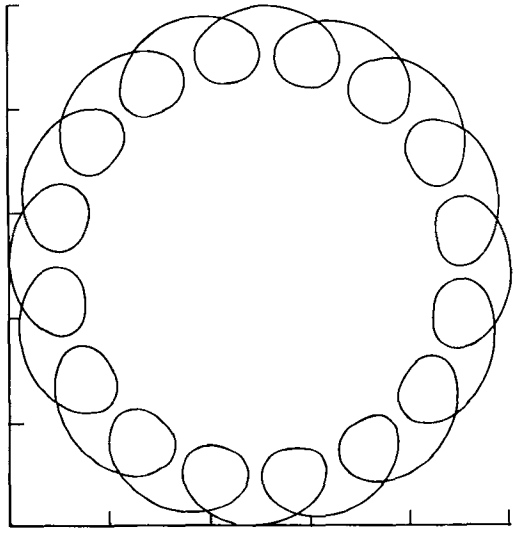

Fig. 7. – Same as fig. 6, but for $\lambda = 100$, $\varrho_0 = 4$, $L = 40.8883$, $\varrho_1 = 3.526$, $\varrho_2 = 4.987$ 21].

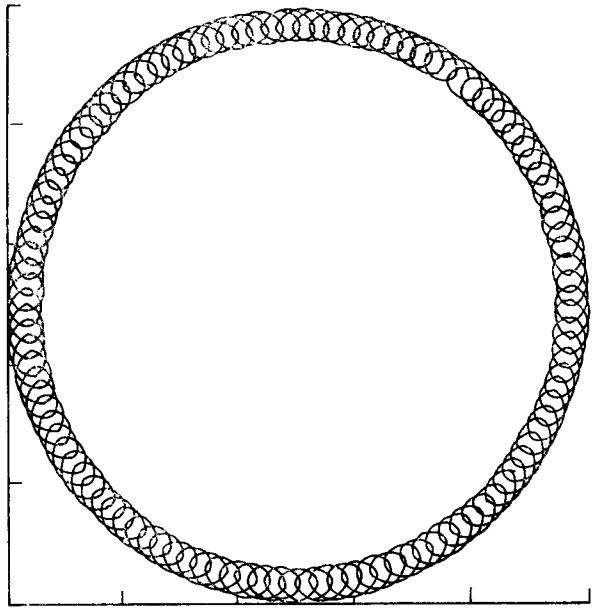

Fig. 8. – Same as fig. 6, but for $\lambda = 100$, $\varrho_0 = 3$, $L = 70.7816$, $\varrho_1 = 2.834$, $\varrho_2 = 3.220$ [21].

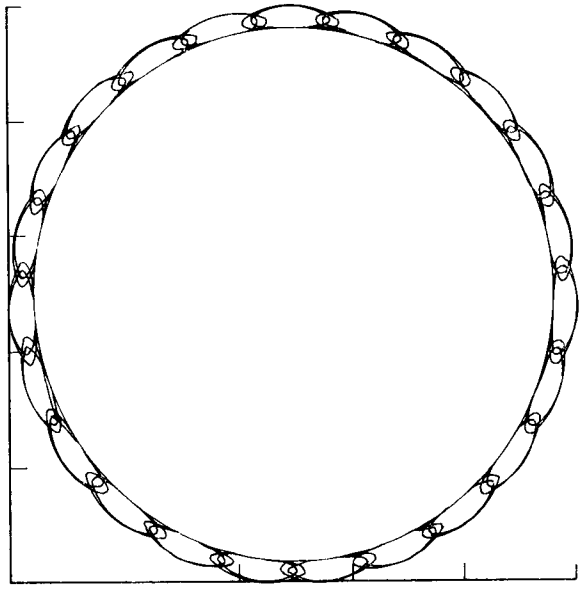

Fig. 9. – Same as fig. 6, but for $E = 3$, $\varrho_0 = 2.1$, $L = 81.2964$, $\varrho_1 = 2.023$, $\varrho_2 = 2.145$ [21].

iv) Finally, if the particle's parameters correspond to the extrema of the potential well, then the particle will execute circular orbits which are stable if they corresponds to the minima, but unstable if they corresponds to the maxima.

The flat minimum which lies far away is just the Schwarzschild potential well and particles here are in a stable orbit only if their energies E is less than 1, as is well known.

In the case in which $L < 0$ there is no potential well near the black hole and thus these particles either plunge into the black hole if they are highly relativistic $E > E_{\max}$ or get scattered away by the magnetic field otherwise.

In order to get the actual orbits, PRASANNA and VARMA have integrated the system of equations (5.7)-(5.9) after using the initial conditions

$$\theta = \frac{\pi}{2}, \qquad \frac{\mathrm{d}\theta}{\mathrm{d}\sigma} = 0, \qquad \varphi_0 = 0, \qquad \varrho = \varrho_0$$

and

$$\text{(5.12)} \qquad \begin{cases} L = -\dfrac{3\lambda\varrho_0^2}{8}\left\{\ln\left(1-\dfrac{2}{\varrho_0}\right)+\dfrac{2}{\varrho_0}\left(1+\dfrac{1}{\varrho_0}\right)\right\}, \\ \left(\dfrac{\mathrm{d}\varrho}{\mathrm{d}\sigma}\right)_0 = (E^2-1+2/\varrho_0)^{\frac{1}{2}}. \end{cases}$$

The results of this integration for different ϱ_0, λ and E are shown in fig. 6 to 9. The important point to notice is the existence of a bound stable orbit very close to the event horizon ($\varrho_0 = 2.1$), unlike the case of the pure Schwarzschild geometry, wherein the last stable orbit exists for $\varrho_0 = 6$.

In the case of the Kerr background geometry the method of approach used by most of the authors (except WALD) while solving Maxwell's equations is the same, wherein they begin with the Newman-Penrose complex tetrad formalism [34] and then use Teukolsky's technique of separation of radial and angular functions [35]. CHITRE and VISHVESHWARA [17] were among the first to discuss the electromagnetic field of a current loop around a Kerr black hole. As they point out, the presence of current loops would produce in addition to the magnetic field an induced electric field due to the rotation of the black hole, which can lead to possible charge accretion. PETTERSON [18], on the other hand, generalizing his earlier studies of current loops around a Schwarzschild black hole to that of Kerr, obtained the expressions for the components of the vector potential in a relatively simple form of a combination of first derivatives of Legendre polynomials. As he points out, while in the Schwarzschild case one could have considered the electric and magnetic fields separately, this cannot be done on the Kerr background as rotation mixes them up. He has further calculated the field of a loop carrying both a current and a net charge in the equatorial plane and also the true minimum-energy configuration of the system in which the black hole and the current loop have equal but opposite net charge rendering the total configuration electrically neutral. Such a neutrality would ensure the stationarity with respect to charge accretion, as no charges will be drawn by the system from infinity. KING *et al.* [19] have

considered the possible stationary axisymmetric electromagnetic fields in a vacuum cavity between an initially neutral black hole and a surrounding plasma shell and conclude that the magnetic field must be uniform to a good approximation except near the shell where higher multipoles could bend the field lines. They find that the flux of magnetic field across one hemisphere of a neutral black hole decreases monotonically from a maximum value at $a = 0$ to zero at the extreme limit $|a| = m$, and the hole tends to accrete charges selectively, like for positive charges over the upper and lower parts of its surface and negative charges in a comparatively narrow band around the equator. CHANDRASEKHAR [36] has given an explicit solution for the vector potential for a stationary axisymmetric electromagnetic field around a Kerr black hole in terms of Teukolsky's radial and angular functions.

WALD [20], on the other hand, making use of the fact that a Killing vector in vacuum space-time serves as a vector potential for a Maxwell test field, has derived the solution for the deformed electromagnetic field, when a Kerr black hole is placed in an originally uniform magnetic field. Strangely he finds no enhancement of the magnetic-field strength near the black hole as one would have expected due to possible sucking in of lines of force by the black hole. However, similarly to the case of a general magnetic field, the rotation induces an electric field in the vicinity of the black hole.

PRASANNA and VISHVESHWARA [22] have studied in detail the trajectories of a charged test particle in a dipole magnetic field superposed on a Kerr background, using the explicit solution of Petterson, and those in an uniform magnetic field on a Kerr background, using Wald's solution. We shall now consider these cases in the following.

By using the usual approach, the constants of the motion, energy and canonical angular momentum for a particle of charge e and mass M_0 may be obtained from (2.9) and (2.10) as

$$u_\varphi + eA_\varphi = l\,, \qquad u_t + eA_t = -E\,, \tag{5.13}$$

from which for the Kerr metric in Boyer-Lindquist co-ordinates

$$\begin{cases} \mathrm{d}s^2 = -\left(1 - \dfrac{2mr}{\Sigma}\right)\mathrm{d}t^2 - \dfrac{4mra}{\Sigma}\sin^2\theta\,\mathrm{d}t\,\mathrm{d}\varphi + \\ \qquad\qquad + (\Sigma/\Delta)\,\mathrm{d}r^2 + \Sigma\,\mathrm{d}\theta^2 + (A/\Sigma)\sin^2\theta\,\mathrm{d}\varphi^2\,, \\ \Sigma = r^2 + a^2\cos^2\theta\,, \qquad \Delta = r^2 + a^2 - 2mr\,, \\ A = (r^2 + a^2)^2 - \Delta a^2\sin^2\theta\,, \end{cases} \tag{5.14}$$

the first integrals u^φ and u^t may be written as

$$u^\varphi \equiv \frac{\mathrm{d}\varphi}{\mathrm{d}s} = \frac{1}{\Delta\sin^2\theta}\left\{\left(1 - \frac{2mr}{\Sigma}\right)(l - eA_\varphi) + \frac{2mra}{\Sigma}\sin^2\theta(E + eA_t)\right\} \tag{5.15}$$

and

$$(5.16)\qquad u^t \equiv \frac{\mathrm{d}t}{\mathrm{d}s} = \frac{1}{\Delta \sin^2\theta}\cdot \cdot\left\{\frac{(r^2+a^2)^2 - \Delta a^2 \sin^2\theta}{\Sigma}\sin^2\theta(E + eA_t) - \frac{2mra}{\Sigma}\sin^2\theta(l - eA_\varphi)\right\}.$$

The equations governing the r- and θ-motion are given by the usual Lorentz equation, which may explicitly be written as

$$(5.17)\qquad \frac{\mathrm{d}^2 r}{\mathrm{d}s^2} - \frac{m(r^2 - a^2\cos^2\theta) - ra^2\sin^2\theta}{\Sigma\Delta}\left(\frac{\mathrm{d}r}{\mathrm{d}s}\right)^2 - \frac{r\Delta}{\Sigma}\left(\frac{\mathrm{d}\theta}{\mathrm{d}s}\right)^2 - - \frac{2a^2\sin\theta\cos\theta}{\Sigma}\frac{\mathrm{d}r}{\mathrm{d}s}\frac{\mathrm{d}\theta}{\mathrm{d}s} + \frac{m\Delta}{\Sigma^3}(r^2 - a^2\cos^2\theta)\left(\frac{\mathrm{d}t}{\mathrm{d}s}\right)^2 - \frac{\Delta\sin^2\theta}{\Sigma^3}\cdot \cdot\{r^5 + 2r^3a^2\cos^2\theta - mr^2a^2\sin^2\theta + ra^4\cos^2\theta + (m-r)a^4\sin^2\theta\cos^2\theta\}\cdot \cdot\left(\frac{\mathrm{d}\varphi}{\mathrm{d}s}\right)^2 - \frac{2\Delta ma\sin^2\theta}{\Sigma^3}(r^2 - a^2\cos^2\theta)\frac{\mathrm{d}\varphi}{\mathrm{d}s}\frac{\mathrm{d}t}{\mathrm{d}s} = \frac{e\Delta}{\Sigma}\left\{A_{\varphi,r}\frac{\mathrm{d}\varphi}{\mathrm{d}s} + A_{t,r}\frac{\mathrm{d}t}{\mathrm{d}s}\right\}$$

and

$$(5.18)\qquad \frac{\mathrm{d}^2\theta}{\mathrm{d}s^2} + \frac{a^2\sin\theta\cos\theta}{\Sigma\Delta}\left(\frac{\mathrm{d}r}{\mathrm{d}s}\right)^2 + \frac{2r}{\Sigma}\frac{\mathrm{d}r}{\mathrm{d}s}\frac{\mathrm{d}\theta}{\mathrm{d}s} - \frac{a^2\sin\theta\cos\theta}{\Sigma}\left(\frac{\mathrm{d}\theta}{\mathrm{d}s}\right)^2 - - \frac{2mra^2}{\Sigma^3}\sin\theta\cos\theta\left(\frac{\mathrm{d}t}{\mathrm{d}s}\right)^2 + \frac{4mra(r^2+a^2)}{\Sigma^3}\sin\theta\cos\theta\cdot \cdot\frac{\mathrm{d}\varphi}{\mathrm{d}s}\frac{\mathrm{d}t}{\mathrm{d}s} - \frac{\sin\theta\cos\theta}{\Sigma^3}[(r^2+a^2)^3 - (r^2+a^2+\Sigma)\Delta a^2\sin^2\theta]\cdot \cdot\left(\frac{\mathrm{d}\varphi}{\mathrm{d}s}\right)^2 = \frac{e}{\Sigma}\left\{A_{\varphi,\theta}\frac{\mathrm{d}\varphi}{\mathrm{d}s} + A_{t,\theta}\frac{\mathrm{d}t}{\mathrm{d}s}\right\}.$$

The general solution of Petterson for the vector potential of the electromagnetic field outside the sources is given by

$$(5.19)\qquad -A_t = \frac{rq}{\Sigma} + \sum_{l=1}^{\infty}\left[\frac{\Delta}{\Sigma}\frac{\mathrm{d}Q_l}{\mathrm{d}r}Q_l(\cos\theta)(r\beta_l^r - a\cos\theta\beta_l^i) + + \frac{a\sin\theta}{\Sigma}Q_l(u)\frac{\mathrm{d}Q_l}{\mathrm{d}\theta}(r\beta_l^i + a\cos\theta\beta_l^r)\right] + \alpha_t$$

and (*)

$$(5.20)\qquad A_\varphi = \frac{arq\sin^2\theta}{\Sigma} + \sum_{l=1}^{\infty}\left[a\sin^2\theta\frac{\Delta}{\Sigma}\frac{\mathrm{d}Q_l}{\mathrm{d}r}Q_l(\cos\theta)(r\beta_l^r - a\cos\theta\beta_l^i) + + \sin\theta\frac{r^2+a^2}{\Sigma}Q_l(u)\frac{\mathrm{d}Q_l}{\mathrm{d}\theta}(a\cos\theta\beta_l^r + r\beta_l^i) - \frac{\Delta\sin\theta}{l(l+1)}\beta_l^i\frac{\mathrm{d}Q_l}{\mathrm{d}r}\frac{\mathrm{d}Q_l}{\mathrm{d}\theta}\right] + \alpha_\varphi,$$

(*) In Petterson's paper in the expression for A_φ ([18], p. 2222, eq. (29)) the Δ associated with the last term is missing.

wherein $u = (r - m)/\sqrt{m^2 - a^2}$, Q_l is the associated Legendre function and q is the electric charge on the black hole. PRASANNA and VISHVESHWARA have considered the special case of a dipole ($l = 1$) magnetic field and set $q = 0$ (uncharged black hole). The constants α_t and α_φ are also chosen to be zero, whereas β_1^i and β_1^r are chosen such that the electric field is zero when $a = 0$ giving $\beta_1^r = 0$ and asymptotically the magnetic field is Lorentzian, which gives $\beta_1^i = \mp 3\mu/2(m^2 - a^2)$, μ being the magnetic-dipole moment.

With these, the components of the vector potential take the form

$$A_t = \frac{-3a\mu}{2\gamma^2 \Sigma} \cdot \left\{ [r(r-m) + (a^2 - mr)\cos^2\theta] \frac{1}{2\gamma} \ln \frac{r - m + \gamma}{r - m - \gamma} - (r - m\cos^2\theta) \right\} \tag{5.21}$$

and

$$A_\varphi = \frac{-3\mu \sin^2\theta}{4\gamma^2 \Sigma} \left\{ (r-m)a^2 \cos^2\theta + r(r^2 + mr + 2a^2) - \right. \\ \left. - [r(r^3 - 2ma^2 + a^2 r) + \Delta a^2 \cos^2\theta] \frac{1}{2\gamma} \ln \frac{r - m + \gamma}{r - m - \gamma} \right\}, \tag{5.22}$$

wherein $\gamma = \sqrt{m^2 - a^2}$, and the dipole moment is taken to be antiparallel to the rotation axis.

The vector potential for the case of black hole in a uniform magnetic field as found by WALD has the components

$$A_t = - B_0 a[1 - (rm/\Sigma)(2 - \sin^2\theta)] \tag{5.23}$$

and

$$A_\varphi = \frac{B_0 \sin^2\theta}{2\Sigma} [(r^2 + a^2)^2 - \Delta a^2 \sin^2\theta - 4ma^2 r], \tag{5.24}$$

wherein B_0 is the magnetic-field strength.

As the discussion of general motion is complicated, following the usual practice, PRASANNA and VISHVESHWARA have considered the motion along the equatorial plane $\theta = \pi/2$. The effective potential for the r-motion in the equatorial plane is given by

$$V_{\text{eff}} = - A_\tau + K/R \tag{5.25}$$

with

$$\begin{cases} K = 2\alpha(L - \bar{A}_\varphi) + \Delta^{\frac{1}{2}} \{\varrho^2 (L - \bar{A}_\varphi)^2 + \varrho R\}^{\frac{1}{2}}, \\ R = \varrho^3 + \alpha^2 \varrho + 2\alpha^2, \qquad \Delta = \varrho^2 - 2\varrho + \alpha^2, \end{cases} \tag{5.26}$$

wherein the dimensionless quantities ϱ, σ, L are used as defined earlier alongwith $\alpha = a/m$, $\tau = ct/m$, $A_\tau = eA_\tau$, $\bar{A}_\varphi = eA_\varphi/m$. Using $\bar{A}_\varphi$ and A_τ appropriately for the two different cases, they have studied the nature of orbits in detail. Figures 10-13 give the effective-potential plots for the case of the dipole field for different values of the parameters. As in the Schwarzschild case also here

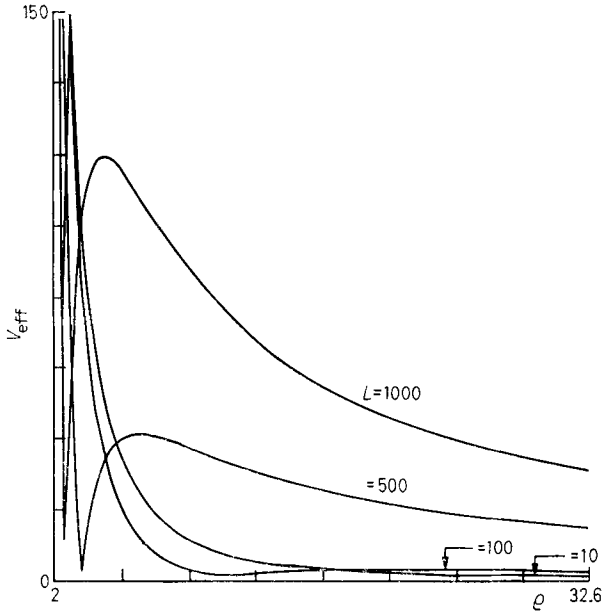

Fig. 10. – Plots of V_{eff} as a function of ϱ for $\alpha = 0.1$, $\lambda = 1000$ for the case of a dipole magnetic field on a Kerr background [22].

there are two maxima and two minima of which the curves present only the first minimum m and the second maximum M_2, due to scaling difficulties. Considering the asymptotic behaviour of V_{eff}, they find that, as $\varrho \to \infty$, $V_{\text{eff}} \to 1$, as $1 - 2/\varrho + \alpha^2/\varrho^2$, a behaviour which is just similar to that of V_{eff} in the pure Kerr geometry. For a given α and λ, as L increases, the centrifugal barrier increases monotonically, whereas the inner maximum M_1 decreases for α up to ≈ 0.45, but it increases for $\alpha > 0.45$. On the other hand, when L is fixed, as λ increases, M_1 increases, whereas m and M_2 keep decreasing monotonically irrespective of the value of α. If L and β are fixed, as α increases the entire potential well moves upwards in energy and towards the event horizon. As $\varrho = 2$ corresponds to the ergosurface in the equatorial plane, it follows that depending on the physical parameters the potential well stays either completely inside or completely outside the ergosurface and in few cases part of it lies inside and part outside the ergosurface.

In the case of the uniform magnetic field the effective potential asymp-

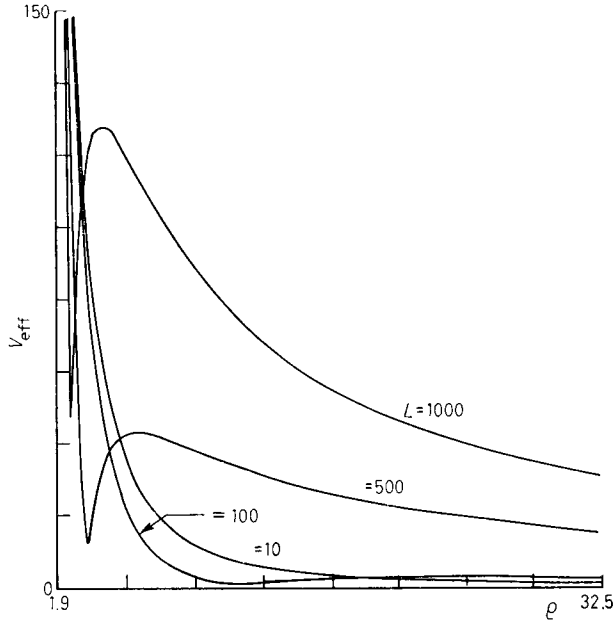

Fig. 11. – Same as fig. 10, but for $\alpha = 0.45$ [22].

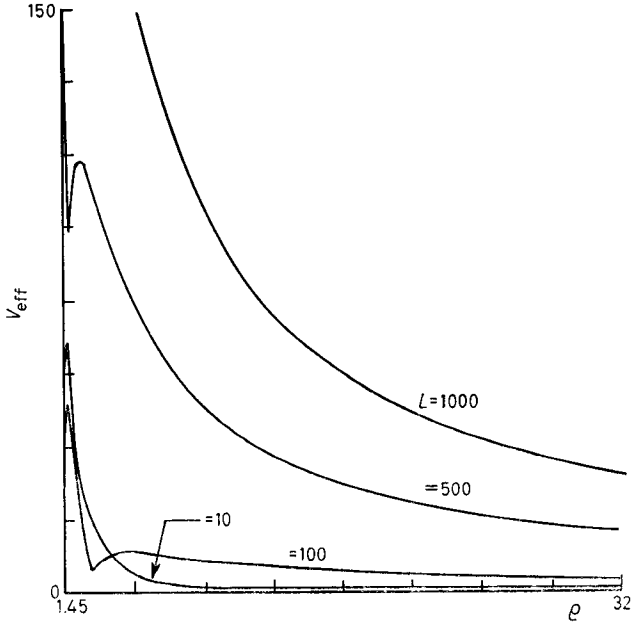

Fig. 12. – Same as fig. 10, but for $\alpha = 0.9$, $\lambda = 150$ [22].

totically goes as

$$\begin{cases} V_{\text{eff}} \approx 1 + \lambda\alpha + (\bar{A}_\varphi)^2/\varrho^2 - (\bar{A}_\varphi L)/\varrho\,, \\ V_{\text{eff}} \approx 1 + \lambda\alpha + \theta(\varrho^2) + \text{constant} \end{cases} \tag{5.27}$$

i.e. as the square of the distance for large ϱ. Unlike the case of dipole magnetic field, here V_{eff} has only one maximum and one minimum both in the vicinity of the black hole, whereas far away from the black hole V_{eff} increases without bound. Thus there always exists a potential well which depending on α, L and λ either lies completely outside the ergosurface or lies partially inside the ergosurface.

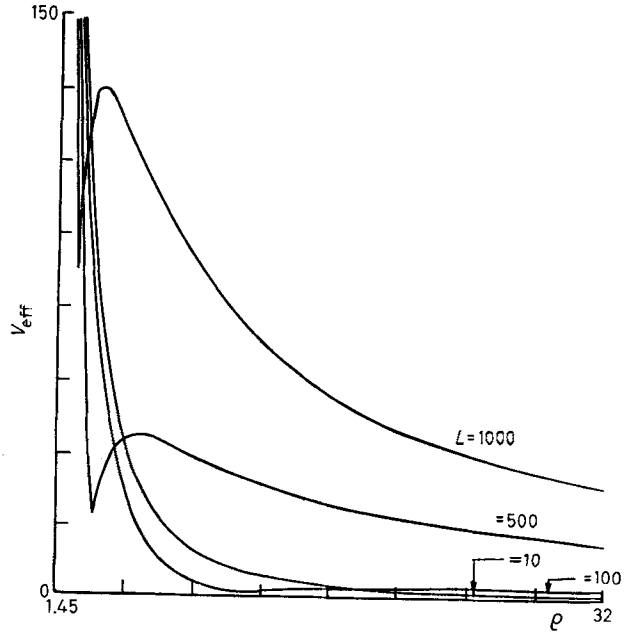

Fig. 13. – Same as fig. 10, but for $\alpha = 0.9$ [22].

From the structure of the potential curves the nature of the orbits are obtained as follows. In the case of the dipole field there are i) plunge orbits for highly relativistic particles with $E > M_1$, ii) unbound orbits for particles coming from infinity with $E < M_1$ or M_2, iii) stable bound gyrating orbits for particles with $E < M_2$ and initially located within the potential well and iv) finally circular orbits stable for $E = (V_{\text{eff}})_{\min}$ and unstable for $E = (V_{\text{eff}})_{\max}$. On the other hand, in the case of a uniform magnetic field, the particle will plunge into the black hole if it is highly energetic, $E > (V_{\text{eff}})_{\max}$, whereas it will gyrate in a bound stable orbit, if $E < (V_{\text{eff}})_{\max}$. As is well known, it will have a circular orbit which is stable if $E = (V_{\text{eff}})_{\min}$ and unstable if $E = (V_{\text{eff}})_{\max}$.

In order to obtain the actual orbits, they integrate the set of equations

$$(5.28)\quad \frac{1}{\Delta}\frac{\mathrm{d}^2\varrho}{\mathrm{d}\sigma^2}-\frac{1}{\Delta^2}\left(1-\frac{\alpha^2}{\varrho}\right)\left(\frac{\mathrm{d}\varrho}{\mathrm{d}\sigma}\right)^2-\left(\frac{1}{\varrho}-\frac{\alpha^2}{\varrho^4}\right)\left(\frac{\mathrm{d}\varphi}{\mathrm{d}\sigma}\right)^2- -\frac{2\alpha}{\varrho^4}\frac{\mathrm{d}\varphi}{\mathrm{d}\sigma}\frac{\mathrm{d}\tau}{\mathrm{d}\sigma}+\frac{1}{\varrho^4}\left(\frac{\mathrm{d}\tau}{\mathrm{d}\sigma}\right)^2=\frac{1}{\varrho^2}\left\{\frac{\mathrm{d}\bar{A}_\varphi}{\mathrm{d}\varrho}\frac{\mathrm{d}\varphi}{\mathrm{d}\sigma}+\frac{\mathrm{d}A_\tau}{\mathrm{d}\varrho}\frac{\mathrm{d}\tau}{\mathrm{d}\sigma}\right\},$$

$$(5.29)\quad \frac{\mathrm{d}\varphi}{\mathrm{d}\sigma}=\frac{1}{\Delta}\left\{\left(1-\frac{2}{\varrho}\right)(L-\bar{A}_\varphi)+\frac{2\alpha}{\varrho}(E+A_\tau)\right\},$$

$$(5.30)\quad \frac{\mathrm{d}\tau}{\mathrm{d}\sigma}=\frac{1}{\Delta}\{(\varrho^2+\alpha^2+2\alpha^2/\varrho)(E+A_\tau)-(2\alpha/\varrho)(L-\bar{A}_\varphi)\}$$

with initial conditions

$$\varphi_0=0\,,\qquad \varrho=\varrho_0\,,$$

$$(5.31)\quad \left(\frac{\mathrm{d}\varrho}{\mathrm{d}\sigma}\right)_0=\pm\left\{\left(1+\frac{\alpha^2}{\varrho_0^2}+\frac{2\alpha^2}{\varrho_0^3}\right)[E+(A_\tau)_0]^2-\left(\frac{1}{\varrho_0^2}-\frac{2}{\varrho_0^3}\right)[L-(\bar{A}_\varphi)_0]^2- -\frac{4\alpha}{\varrho_0^3}[E+(A_\tau)_0][L-(\bar{A}_\varphi)_0]-\left(1-\frac{2}{\varrho_0}+\frac{\alpha^2}{\varrho_0^2}\right)\right\}^{\frac{1}{2}},$$

wherein $(\bar{A}_\varphi)_0$ and $(A_\tau)_0$ refer to values of $\bar{A}_\varphi$ and A_τ at $\varrho=\varrho_0$.

Figures 14*a* to *c* give the bound orbits for the case of the dipole magnetic field, whereas 15*a* to *d* give the orbits in the case of uniform magnetic field.

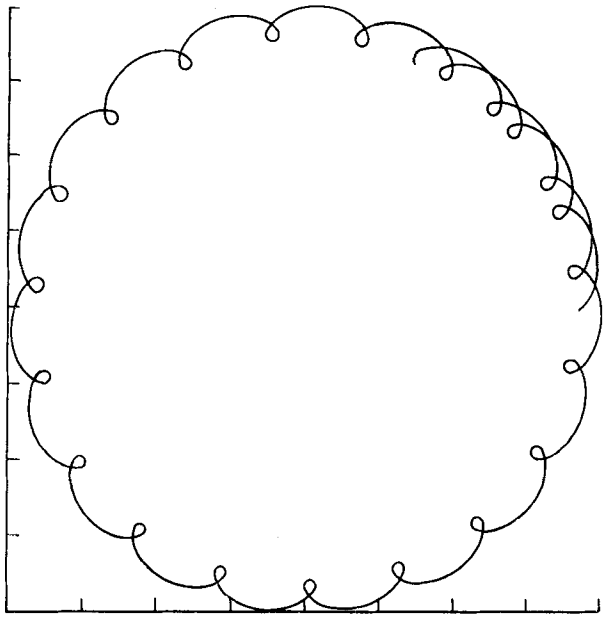

Fig. 14*a*. – Orbits in the equatorial plane in the dipole magnetic field on a Kerr background [22] for $\alpha=0.99$, $\lambda=1000$, $L=500$, $E=30$, $\varrho_0=3.51763$, $\varrho_1=3.39123$, $\varrho_2=3.81977$.

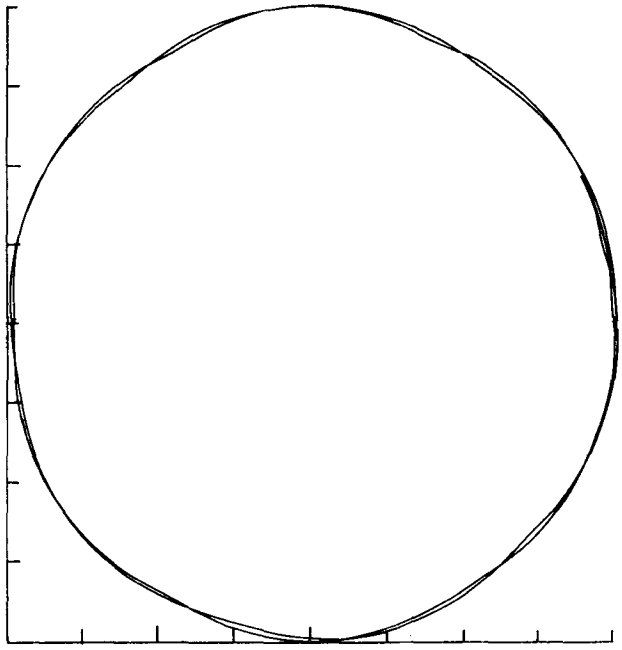

Fig. 14*b*. – Same as fig. 14*a*, but for $\lambda = 50$, $E = 152$, $\varrho_0 = 1.36570$, $\varrho_1 = 1.35715$, $\varrho_2 = 1.39003$ [22].

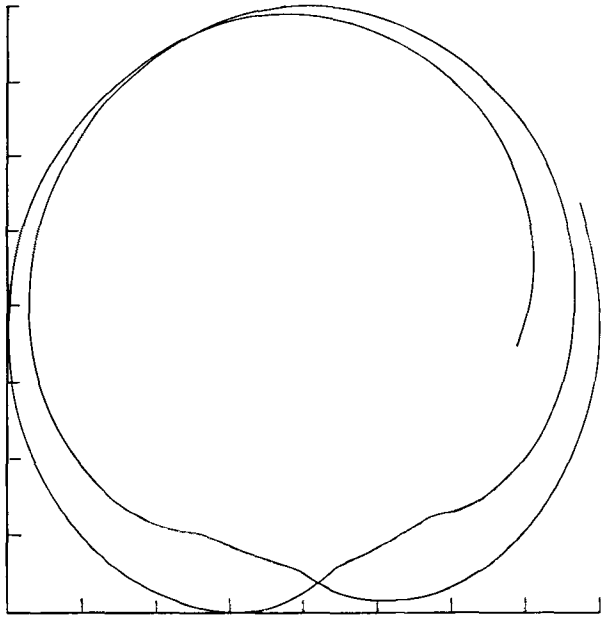

Fig. 14*c*. – Same as fig. 14*a*, but for $\alpha = 0.45$, $E = 158$, $\varrho_0 = 2.13311$, $\varrho_1 = 1.93331$, $\varrho_2 = 3.11145$ [22].

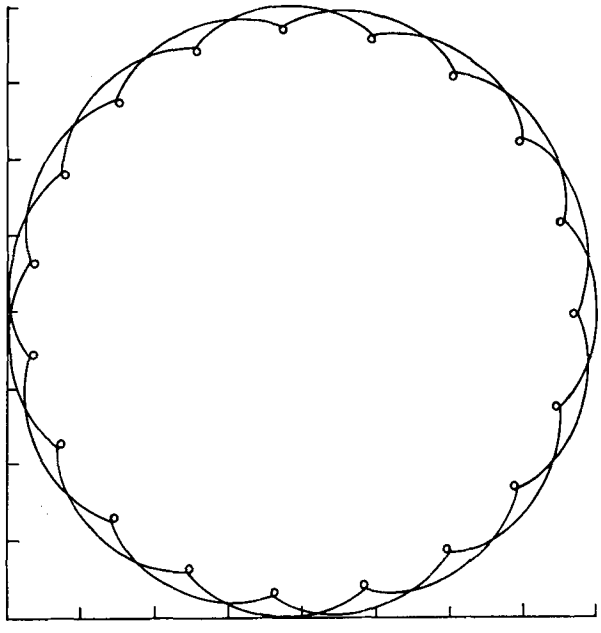

Fig. 14*d*. – Same as fig. 14*a*, but for $\alpha = 0.45$, $\lambda = 500$, $L = 1000$, $E = 100$, $\varrho_0 = 2.13311$, $\varrho_1 = 2.06173$, $\varrho_2 = 2.26142$ [22].

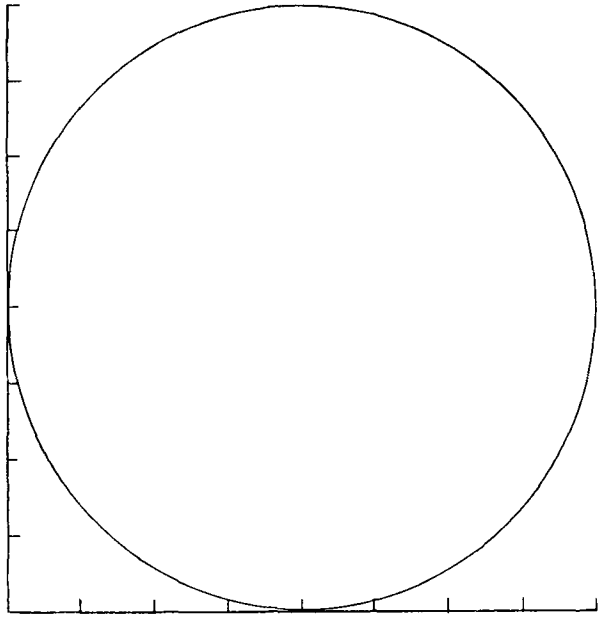

Fig. 14*e*. – Same as fig. 14*a*, but for $\alpha = 0.45$, $\lambda = 500$, $L = 1000$, $E = 72$, $\varrho_0 = 2.13311$, $\varrho_1 = 2.12822$, $\varrho_2 = 2.13963$ [22].

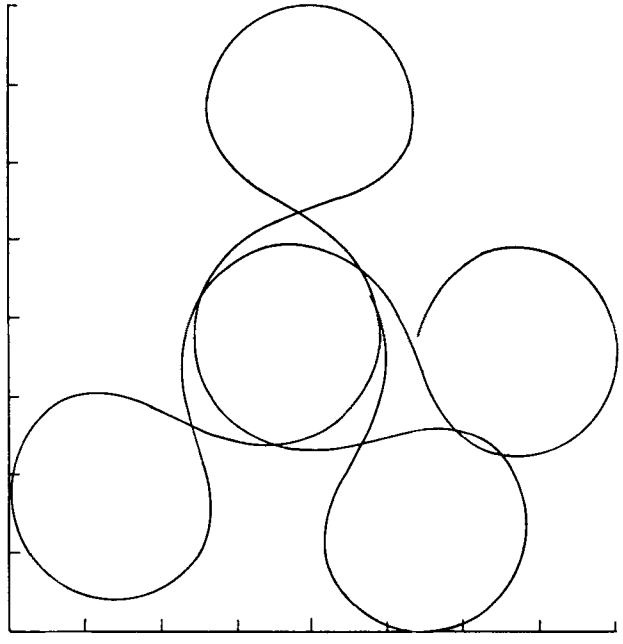

Fig. 15*a*. – Orbits in the equatorial plane in a uniform magnetic field on a Kerr background for $\alpha=0.99$, $\lambda=150$, $L=1000$, $E=350$, $\varrho_0=2.37979$, $\varrho_1=1.72675$, $\varrho_2=6.07672$ [22].

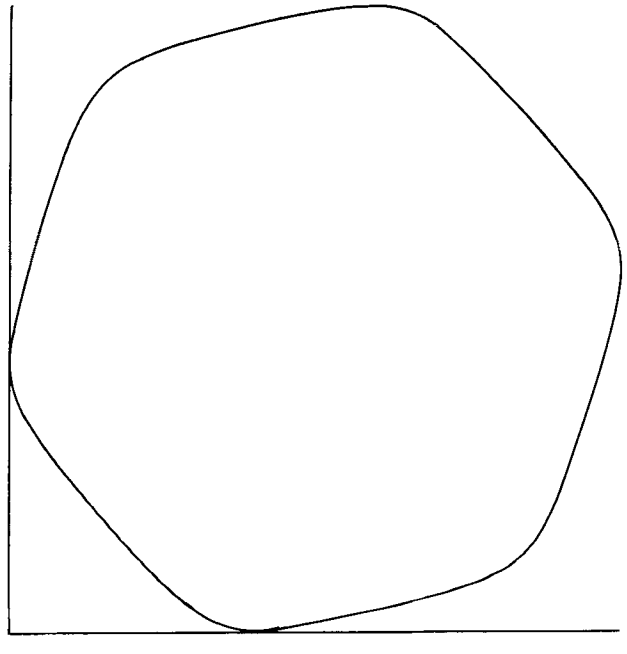

Fig. 15*b*. – Same as fig. 15*a*, but for $\lambda=1000$, $\varrho_0=1.54210$, $\varrho_1=1.48561$, $\varrho_2=1.60200$ [22].

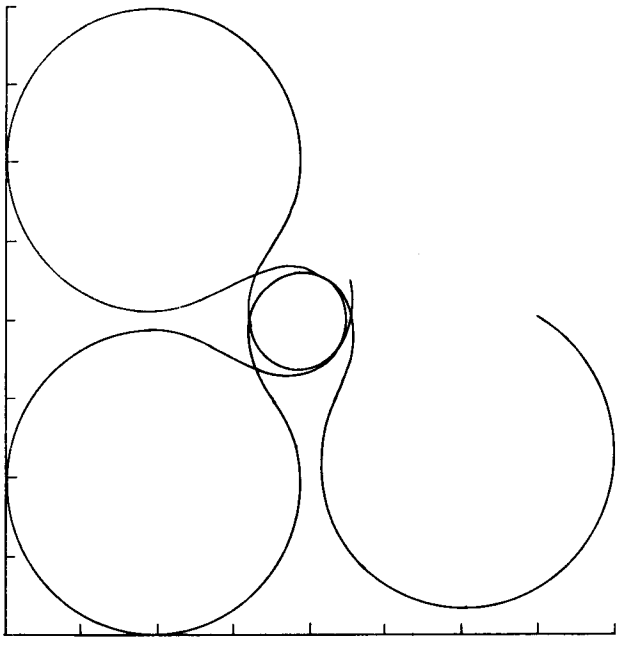

Fig. 15*c*. – Same as fig. 15*a*, but for $\alpha = 0.9$, $\lambda = 50$, $E = 320$, $\varrho_0 = 10$, $\varrho_1 = 1.90970$, $\varrho_2 = 14.7571$ [22].

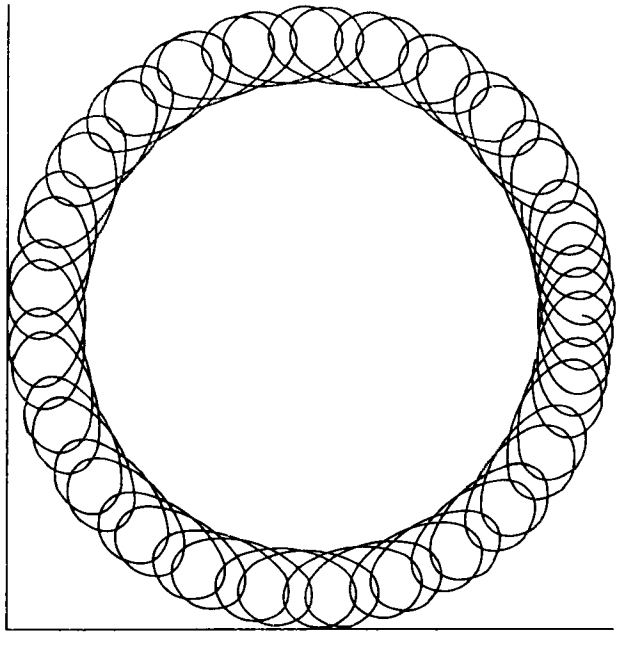

Fig. 15*d*. – Same as fig. 15*a*, but for $\alpha = 0.9$, $E = 150$, $\varrho_0 = 3.65400$, $\varrho_1 = 3.13043$, $\varrho_2 = 4.15418$ [22].

The striking features common to both cases is that the particle executes Larmor motion (gyration) only if it is completely outside the ergosurface during its motion. As PRASANNA and VISHVESHWARA conclude, this is indeed the effect of inertial frame dragging of Kerr geometry. Gyration requires that during every Larmor circle the particle angular velocity $\mathrm{d}\varphi/\mathrm{d}\sigma$ be prograde for one half and retrograde for the other half with respect to the rotation of the black hole. Since the ergosurface in the Kerr geometry is the static limit surface on and behind which no retrograde motion is possible, the particle can gyrate only outside the ergosurface. One can see this analytically as follows. If the particle has to exhibit gyration, it should satisfy two conditions:

$$\left(\frac{\mathrm{d}\varphi}{\mathrm{d}\sigma}\right)_{\varrho_g} = 0\,, \qquad \left(\frac{\mathrm{d}\varrho}{\mathrm{d}\sigma}\right)^2_{\varrho_g} > 0\,.$$

These two conditions together require

$$\left(1-\frac{2}{\varrho_g}\right)^{-1}[E + (A_\tau)_{\varrho=\varrho_g}]^2 > 1\,, \tag{5.32}$$

which can be true only for $\varrho_g > 2$, *i.e.* outside the ergosurface. The actual plots show that when α and L are kept constant the change in orbits may be brought about by changing either the magnetic field (λ) or the energy (E). In fig. 14*a* when $\lambda = 1000$ both the turning points of the orbit lie outside $\varrho = 2$ and thus there is gyration, whereas as λ is decreased to 150 (fig. 14*b*) both the turning points are inside $\varrho = 2$ and thus the particle does not gyrate. On the other hand, in fig. 14*c* and *d* α, L and λ are the same, but E varies. When E is large, the particle moves in and out of the ergosurface without gyrating, but, as the energy is decreased, it is trapped in a region completely outside the ergosurface and thus it gyrates. As the energy is further decreased towards the minimum of V_{eff}, the particle tends to execute an almost circular motion as shown in fig. 14*c* as at $(V_{\mathrm{eff}})_{\mathrm{min}}$ the orbit should be perfectly circular. Figures 15*a-d* depict similar features in the case of uniform magnetic field.

The fact that the nongyration of the particle inside ergosphere is an effect of inertial frame dragging has been further conclusively verified by PRASANNA and CHAKRABORTY [23], who have discussed the particle orbits in the equatorial plane of the Kerr geometry in a locally nonrotating frame (LNRF) for the same vector potentials and the same physical parameters as discussed in [22].

If $u^{\hat{i}}$ represents the velocity four-vector in the LNRF, it is related to the four-velocity u^i in the Boyer-Linquist co-ordinate frame through the relation

$$u^{\hat{i}} = e^{\hat{i}}_j u^j\,, \tag{5.33}$$

wherein

$$e^{\hat{i}}{}_{j} = \begin{bmatrix} (\Sigma\Delta/A)^{\frac{1}{2}} & 0 & 0 & 0 \\ 0 & (\Sigma/\Delta)^{\frac{1}{2}} & 0 & 0 \\ 0 & 0 & \Sigma^{\frac{1}{2}} & 0 \\ -\dfrac{2mar\sin\theta}{\Sigma^{\frac{1}{2}}A^{\frac{1}{2}}} & 0 & 0 & \left(\dfrac{A}{\Sigma}\right)^{\frac{1}{2}}\sin\theta \end{bmatrix}. \tag{5.34}$$

Using similar transformation for F_{ij} and $\Gamma^{i}{}_{jk}$, PRASANNA and CHAKRABORTY obtain the complete set of equations for the motion in the equatorial plane in terms of ϱ, α, σ, A_τ and $\bar{A}_\varphi$ as defined earlier, given by

$$\begin{aligned} \frac{\varrho}{\Delta^{\frac{1}{2}}}\frac{\mathrm{d}^2\varrho}{\mathrm{d}\sigma^2} = \frac{1}{B}\Bigg\{\Delta^{\frac{1}{2}}\left(1-\frac{\alpha^2}{\varrho^3}\right)\left(\frac{\mathrm{d}\varphi}{\mathrm{d}\sigma}\right)^2 + \frac{2\alpha}{\varrho}\left(3+\frac{\alpha^2}{\varrho^2}\right)\frac{\mathrm{d}\varphi}{\mathrm{d}\sigma}\frac{\mathrm{d}\tau}{\mathrm{d}\sigma} - \\ -\frac{1}{\varrho^3\Delta^{\frac{1}{2}}}[(\varrho^2+\alpha^2)^2-4\alpha^2\varrho]\left(\frac{\mathrm{d}\tau}{\mathrm{d}\sigma}\right)^2\Bigg\} + \\ + \frac{1}{\varrho B^{\frac{1}{2}}}\left\{\Delta^{\frac{1}{2}}\bar{A}_{\varphi,\varrho}\frac{\mathrm{d}\varphi}{\mathrm{d}\sigma} + \frac{2\alpha}{\varrho}\bar{A}_{\varphi,\varrho}\frac{\mathrm{d}\tau}{\mathrm{d}\sigma} + BA_{\tau,\varrho}\frac{\mathrm{d}\tau}{\mathrm{d}\sigma}\right\} - \frac{1}{\Delta^{\frac{1}{2}}}\left\{1-\frac{\varrho(\varrho-1)}{\Delta}\left(\frac{\mathrm{d}\varrho}{\mathrm{d}\sigma}\right)^2\right\}, \end{aligned} \tag{3.35}$$

$$\frac{\mathrm{d}\varphi}{\mathrm{d}\sigma} = (L-\bar{A}_\varphi)/B^{\frac{1}{2}}, \tag{5.36}$$

$$\frac{\mathrm{d}\tau}{\mathrm{d}\sigma} = \frac{1}{B\Delta^{\frac{1}{2}}}\left[B(E+A_\tau) - \frac{2\alpha}{\varrho}(L-\bar{A}_\varphi)\right] \tag{5.37}$$

with

$$B = \varrho^2+\alpha^2+2\alpha^2/\varrho\,, \qquad \Delta = \varrho^2-2\varrho+\alpha^2\,.$$

As the $u^{\hat{\varrho}}$ component differs from u^{ϱ} only by a nonzero factor, the effective potential obtained from $u^{\hat{\varrho}} = 0$ is the same as in the earlier case and thus the turning points for any orbit are the same as obtained earlier. Similarly as the effect of change in frame for the electromagnetic field was taken through F_{ij}, the components of the vector potential remain the same as in (5.21)-(5.24), but with $\theta = \pi/2$. Considering the same parameters of bound orbits as in [22], PRASANNA and CHAKRABORTY integrate the system (5.35) to (5.37) and have found that the particle gyrates in all cases, whether it is inside or outside the ergosurface. Figures 16*a-d* show four typical plots of which fig. 16*a* and *b* refer to the dipole case, whereas fig. 16*c* and *d* refer to the uniform-field case. The physical parameters in the case of fig. 16*a* and *d* are same as those of fig. 14*b* and 15*d*, one depicting motion completely inside and the other completely outside the ergosurface.

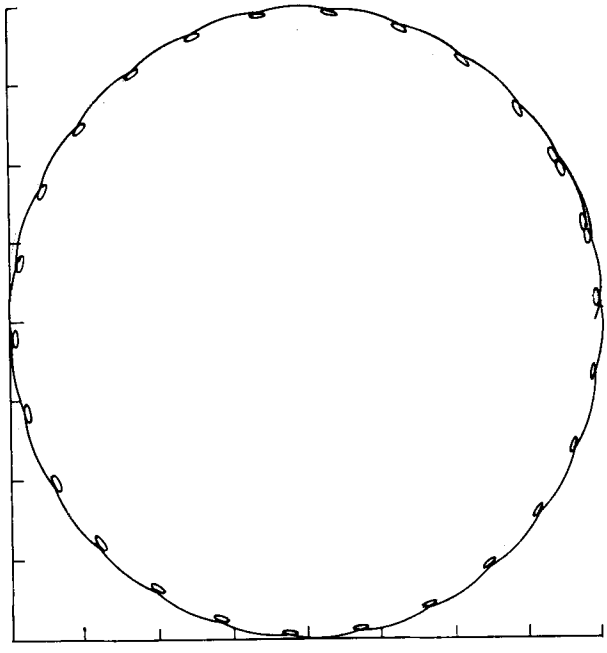

Fig. 16*a*. – Orbits in dipole and uniform magnetic fields on a Kerr background as viewed from a locally nonrotating frame for $\alpha = 0.99$, $\lambda = 50$, $L = 500$, $E = 152$, $\varrho_0 = 1.36570$, $\varrho_1 = 1.35715$, $\varrho_2 = 1.39003$ [23].

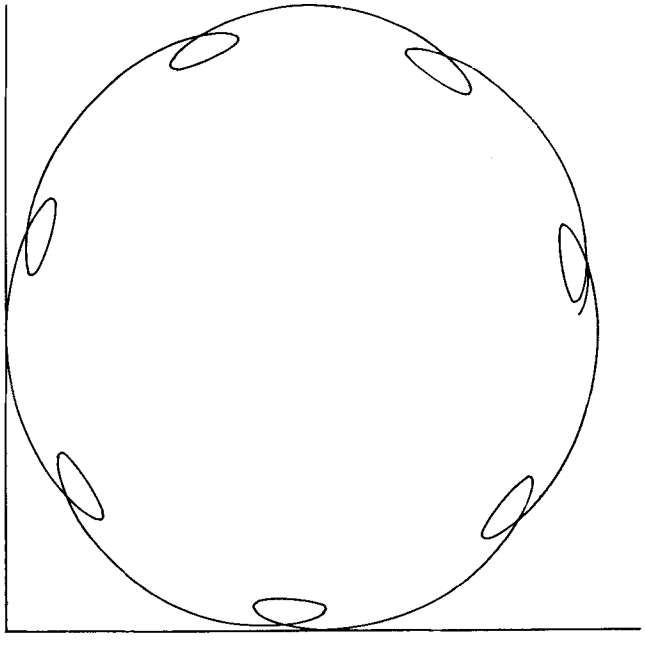

Fig. 16*b*. – Same as fig. 16*a*, but for $\lambda = 1000$, $E = 30$, $\varrho_0 = 3.51763$, $\varrho_1 = 3.39123$, $\varrho_2 = 3.81775$ [23].

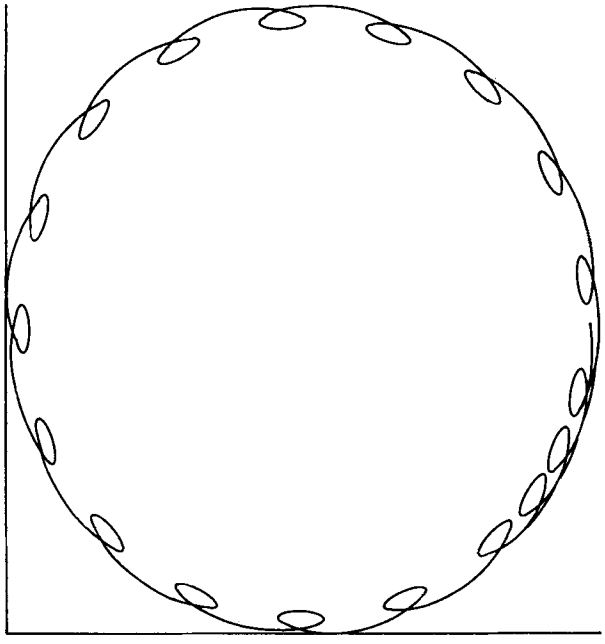

Fig. 16*c*. – Same as fig. 16*a*, but for $\lambda = 1000$, $L = 1000$, $E = 350$, $\varrho_0 = 1.54210$, $\varrho_1 = 1.48561$, $\varrho_2 = 1.60200$ [23].

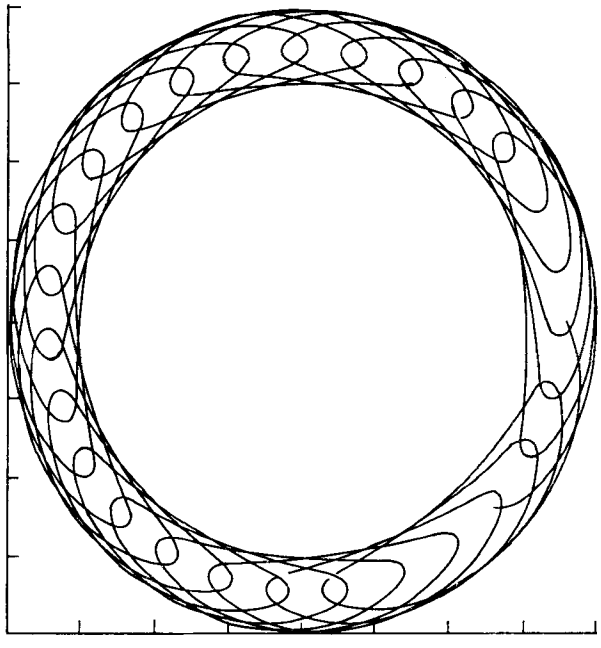

Fig. 16*d*. – Same as fig. 16*a*, but for $\alpha = 0.9$, $\lambda = 150$, $E = 150$, $\varrho_0 = 3.65400$, $\varrho_1 = 3.13043$, $\varrho_2 = 4.15248$ [23].

6. – Motion in the static Ernst space-time.

ERNST [37] has shown that the stationary axisymmetric solution of the Einstein-Maxwell equations can be generated from a pair of complex potentials χ and ψ satisfying the equations

$$\begin{cases} (\mathrm{Re}\,\chi + |\psi|^2)\,\nabla^2\chi = (\nabla\chi + 2\psi * \nabla\psi)\cdot\nabla\chi\,, \\ (\mathrm{Re}\,\chi + |\psi|^2)\,\nabla^2\psi = (\nabla\chi + 2\psi * \nabla\psi)\cdot\nabla\psi \end{cases} \tag{6.1}$$

and subsequently KINNERSLEY identified an invariance group of these equations which was later extended by KINNERSLEY and CHITRE [7] to which we referred in the introduction; ERNST [38] using this technique obtained some solutions representing black holes in a magnetic universe. Though these solutions of Ernst have nonsingular event horizons, they lack the very important criterion of asymptotic flatness, as we mentioned earlier. However, as the Universe as a whole is considered to be homogeneous and isotropic, one is not too wrong if one violates asymptotic flatness for reasonable physical solutions. DADHICH, HOENSELAERS and VISHVESHWARA have studied [39] the trajectories of charged particles in the static Ernst space-time which is also considered as a solution for a Schwarzschild black hole immersed in Melvin's magnetic universe.

Ernst space-time is given by

$$\mathrm{d}s^2 = F^2\left[-\left(1-\frac{2m}{r}\right)\mathrm{d}t^2 + \left(1-\frac{2m}{r}\right)^{-1}\mathrm{d}r^2 + r^2\,\mathrm{d}\theta^2\right] + (r^2\sin^2\theta/F^2)\,\mathrm{d}\varphi^2 \tag{6.2}$$

with $F = 1 + B^2 r^2 \sin^2\theta$, B being the magnetic field along the axis. As may be easily seen, this metric reduces to that of Schwarzschild for $B = 0$ and to that of Melvin's magnetic universe for $m = 0$. When $|Bm| \ll 1$, outside the horizon in the region $2m \ll r \ll B^{-1}$ the space is approximately flat and the magnetic field is approximately uniform. However, if the magnetic field is strong, say of the order $1/m$, then there would be no region outside the event horizon where the magnetic field may be considered uniform.

DADHICH *et al.* have obtained the charged-particle trajectories, using the Hamilton-Jacobi equation, as was done by CARTER for Kerr-Newman space-time and by MELVIN [32] for the case of Melvin's magnetic universe. They obtain the energy and the axial angular momentum as given by

$$E = F^2(1 - 2m/r)\,u^t \tag{6.3}$$

and

$$l = r^2\sin^2\theta\,u^\varphi + e\Phi\,, \tag{6.4}$$

wherein Φ is the electric potential with respect to the angular Killing vector ζ^i given by

$$\Phi = A_i \zeta^i = Br^2 \sin^2\theta/F\,, \tag{6.5}$$

A_i being the vector potential.

Though the general Hamilton-Jacobi equation is not separable from symmetry considerations, they find that for the motion confined to the equatorial plane the equation is separable and the Jacobi action is given by

$$S = S(r) + l\varphi - Et - \tfrac{1}{2}s\,, \tag{6.6}$$

wherein s represents the proper time and

$$S(r) = \int \frac{(E^2 - R)^{\frac{1}{2}}}{1 - 2m/r}\,\mathrm{d}r\,. \tag{6.7}$$

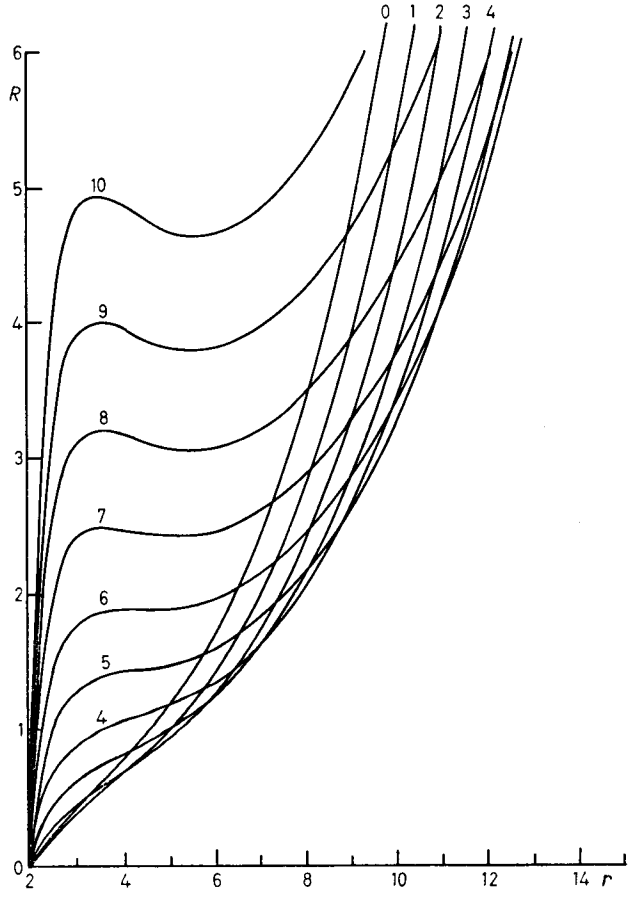

Fig. 17. – Effective-potential plot for static Ernst space-time with $B = 0.1$, $e = 1$ and for various values of l [39].

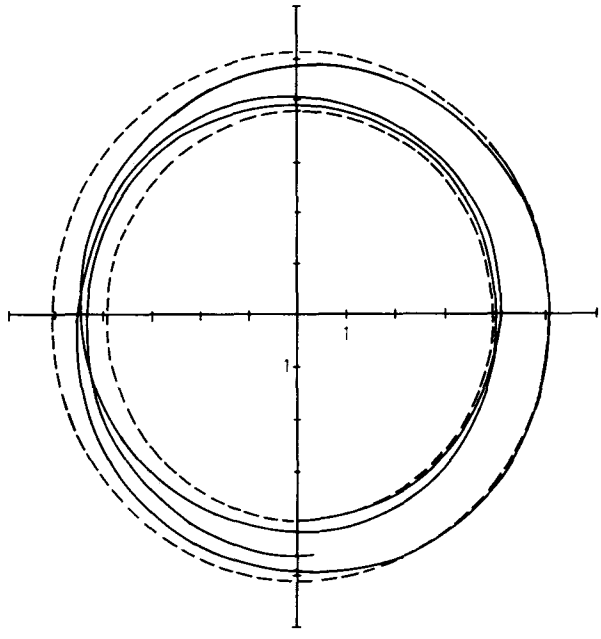

Fig. 18. – A bound orbit in the Ernst field with parameters $l = 6$, $B = 0.1$, $e = 1$, $E^2 = 1.881$ [39].

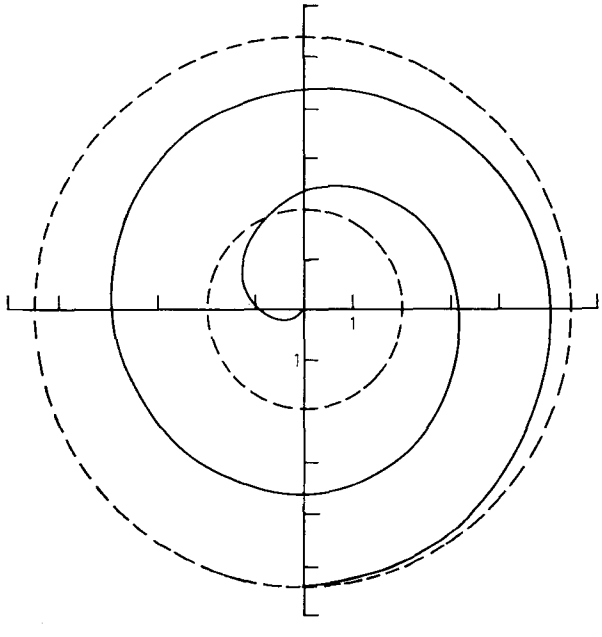

Fig. 19. – A capture orbit in the Ernst field with parameters $l = 6$, $B = 0.1$, $e = 1$, $E^2 = 1.9$ [39].

Here R denotes the « effective potential » for the r-motion given by

$$R = F^2(1 - 2m/r)[1 + (F^2/r^2)(l - e\Phi)^2]\,. \tag{6.8}$$

As S has to be real, (6.7) obviously implies $E^2 \geqslant R$. The orbits themselves they obtain by quadratures, as, for example,

$$\varphi = \int \frac{F^4(l - e\Phi)}{r^2(E^2 - R)^{\frac{1}{2}}}\,\mathrm{d}r\,. \tag{6.9}$$

Figure 17 gives a plot of the effective potential as a function of r. For the parameters used they find that there are no potential wells for $l < 5$ and thus these particles plunge into the black hole, whereas with $l \geqslant 5$ the well exists and deepens as l increases. As was found by PRASANNA and VARMA for the dipole field on the Schwarzschild background, in this case too stable orbits exist for $r < 6m$. Figures 18 and 19 show two typical plots of the orbits as obtained by DADHICH *et al.* As may be seen from fig. 18, in the case of bound orbit the particle gyrates, but the Larmor circle is as large as the orbit itself.

7. – Discussion and conclusions.

An important feature associated with the particle motion is the possible radiation emission. In flat space-time a particle moving with relativistic speed ($V \sim c$) in circular orbits emits synchrotron radiation. It is possible that curved background could modify such emissions. Further, a charged particle moving in a combined gravitational and electromagnetic field could possibly emit both gravitational and electromagnetic radiation [40]. RUFFINI [41] has given a relativistic treatment of the brehmsstrahlung radiation from a charged particle moving in a static gravitational field assuming that the particle and the emitted radiation do not change the background geometry and that there is no radiation reaction. His main conclusions are the following.

i) If the background geometry is that of Schwarzschild and if the freely falling particle has its initial energy equal to its rest mass, then 90 % of the radiation is dipolar in nature, while the contributions from higher multipoles are negligibly small. The total amount of radiation emitted is $\Delta E \approx 2 \cdot 10^{-2} e^2/m$, with the peak of the spectrum at $\omega = 0.2/m$. If the initial energy is greater than the rest mass energy, the amount of energy radiated increases and the contributions from higher multipoles are not negligible. For $E = 1.4m$ the total energy emitted is $\Delta E = 6 \cdot 10^{-2} e^2/m$ and the quadrupole contribution is approximately $\frac{1}{3}$ of the dipole contribution. Consequently the peak of the distribution shifts towards higher frequencies.

ii) If the background geometry is that of Reissner-Nordström, for a charged particle with $e < 0$, the amount of energy radiated increases substantially compared to the other case and the contributions from higher multipoles are predominant. For $Q = 0.95m$ and $e = 50$, $\Delta E = e^2/m$, and the peak of the spectrum is largely displaced towards higher frequencies. Figures 20 and 21 show schematic diagrams of the spectrum for Schwarzschild and Reissner-Nordström geometries.

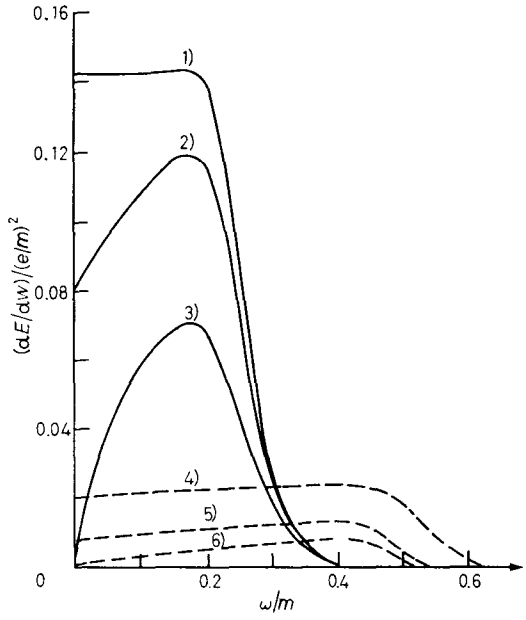

Fig. 20. – Spectrum of the electromagnetic energy radiated by a particle falling into a Schwarzschild black hole for selected values of E_∞ for the dipole (1)-3)) and quadrupole (4)-6)) term of the radiation [41]: 1) $r = 1.4$, 2) $r = 1.2$, 3) $r = 1.0$, 4) $r = 1.4$, 5) $r = 1.2$, 6) $r = 1.0$.

RUFFINI and ZERILLI [26] have considered the radiation emitted by particles in ultra-relativistic circular orbits in the Reissner-Nordström background. They find that the spectrum of the radiation emitted rapidly recovers the main features of synchrotron radiation in flat space as the orbits move outwards with the increase in the absolute value of the test charge. When the particle is near $r_{\min}$, the peak of the potential barrier, the highest multipoles are maximally affected and very much damped, whereas damping in the dipole term is very small. In their opinion the reason for this anomalous behaviour of the spectrum of radiation for orbits near $r_{\min}$ is due to the fact that the radiation originates in a region very near the photon circular orbit which is also at $r_{\min}$ and that large amounts of energy are lost to the black hole. Naturally these effects diminish for orbits which are far away from the black hole (event horizon).

The analysis as made by RUFFINI and co-workers for radiation from charged particles in static geometries has not yet been extended to the case of charged-particle motion in electromagnetic fields superposed on curved geometries. As far as the orbits are concerned, it has been found by PRASANNA *et al.* [21-23] that stable orbits exist for particles even very close to the event horizon if their energy and angular momentum are right. In these curved geometries (Schwarzschild and Kerr's), when there is no magnetic field, the

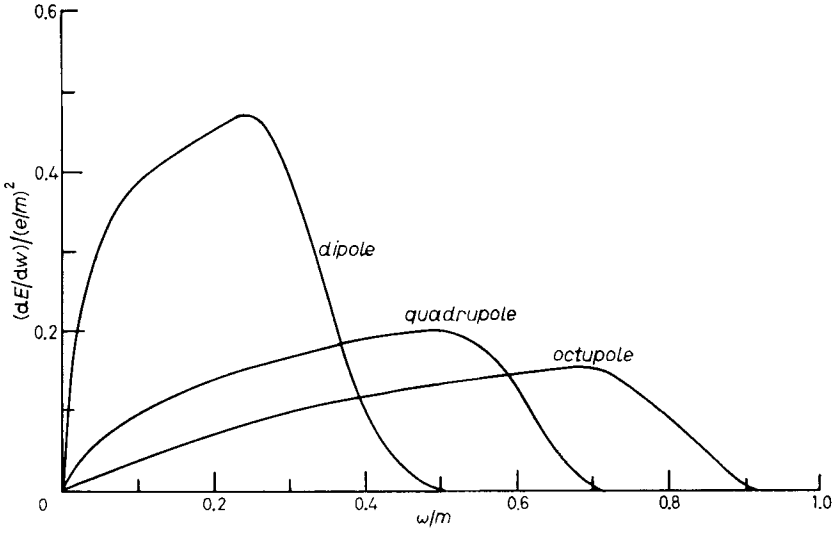

Fig. 21. – Energy spectrum for a charge $e = -50$, falling into an almost extreme Reissner-Nordström geometry $Q = 0.95\,m$ for selected values of the multipoles [41].

particle will be in bound orbit only if its energy is less than its rest mass ($E < 1$). But, as the superposition of a magnetic field changes the structure of the potential curve and introduces a potential well very near to the event horizon, particles can now be trapped in this well in bound orbits. As indicated earlier, the two maxima that occur for the « effective potential » are, respectively, due to the magnetic field and the canonical angular momentum (giving rise to centrifugal barrier). Figure 22 gives a typical plot of the two maxima and the inner minimum as a function of L for a given λ, in the case of a dipole field on a Schwarzschild background [21]. As may be seen from this plot for any λ, there is always a value of L for which the two maxima are equal, corresponding to which the potential well is deepest, and in this potential well now particles with energy much greater than their rest mass can be trapped in the barrier created by its angular momentum and the magnetic field.

PRASANNA and VARMA [21] have also discussed the particle motion off the equatorial plane by integrating (numerically) the complete set of equations

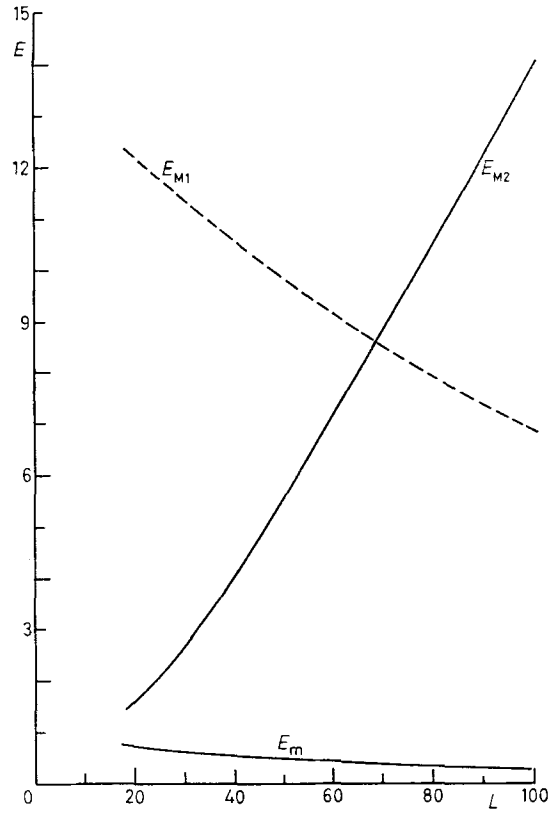

Fig. 22. – Plots of V_{eff} maxima and minimum against L for the value $\lambda = 50$ for the case of a charged particle in a dipole magnetic field superposed on a Schwarzschild geometry [21].

(5.7)-(5.10) for the initial conditions

$$\varrho = \varrho_0\,, \qquad \theta_0 = \pi/2\,, \qquad \varphi_0 = 0\,,$$

$$\text{(7.1)} \qquad \begin{cases} \left(\dfrac{\mathrm{d}\varrho}{\mathrm{d}\sigma}\right)_0 = \pm\left\{E^2 - \left(1 - \dfrac{2}{\varrho_0}\right)\left[1 + \varrho_0^2\left(\dfrac{\mathrm{d}\theta}{\mathrm{d}\sigma}\right)_0^2\right]\right\}^{\frac{1}{2}}, \\ \left(\dfrac{\mathrm{d}\theta}{\mathrm{d}\sigma}\right)_0^2 < \dfrac{E^2}{\varrho_0^2}\left(1 - \dfrac{2}{\varrho_0}\right)^{-1} - \dfrac{1}{\varrho_0^2}, \\ \left(\dfrac{\mathrm{d}\varphi}{\mathrm{d}\sigma}\right)_0 = 0 \Rightarrow L = -\dfrac{3\lambda\varrho_0^2}{8}\left[\ln\left(1 - \dfrac{2}{\varrho_0}\right) + \dfrac{2}{\varrho_0}\left(1 + \dfrac{1}{\varrho_0}\right)\right] \end{cases}$$

by specifying λ, E, ϱ_0 and $(\mathrm{d}\theta/\mathrm{d}\sigma)_0$. A typical plot of this motion is shown in fig. 23. If the magnetic field is large, the motion looks similar to that in the flat geometry, wherein the particle gyrates in a given tube of lines reflecting between two mirror points located symmetrically with respect to the equatorial plane. On the other hand, if the magnetic field is lower, then the par-

ticle oscillations up and down the equatorial plane damp continuously as r decreases and eventually the particle gets sucked in by the black hole.

The review made above deals essentially with the motion of charged particles in electromagnetic fields superposed on a curved background. As maintained in the introduction these electromagnetic fields do not affect the underlying geometry. With such an assumption the question that would arise is about the origin of such fields. Basically there could be three types of such

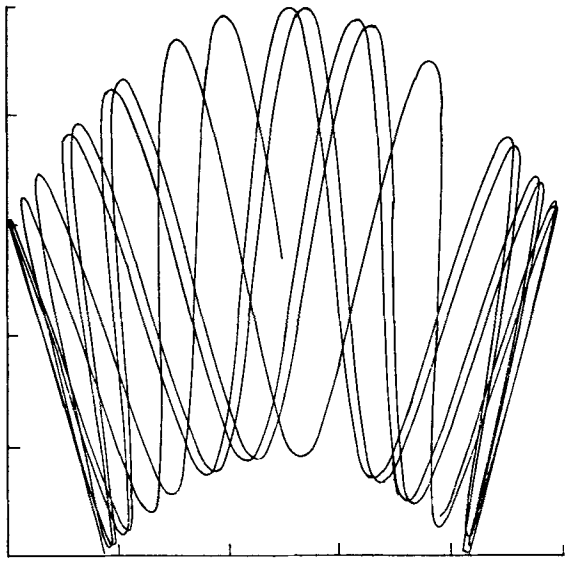

Fig. 23. – Projection of the (ϱ, θ) oscillatory motion of a positively charged particle indicating reflection at mirror points [21], $E = 2$, $\lambda = 100$, $\varrho_0 = 3$, $\mathrm{d}\theta/\mathrm{d}\sigma = 0.3$, $L = 70.7816$.

fields: i) one that arises due to rotation of the compact object carrying either charge or a dipole type of magnetic field, ii) another one due to current loops that form in the vicinity of the black hole, due to motion of charged particles, and iii) the intergalactic and interstellar fields in which the black hole is assumed to be immersed.

The Kerr-Newmann geometry essentially treats the field due to a rotating charged body. On the other hand, RUFFINI and TREVES [42] have considered the fields due to a magnetized rotating sphere. They show that purely on energetic grounds a magnetized rotating object should indeed be expected to possess a nonzero net charge. However, due to the well-known «no hair theorem» of black-hole physics, it is clear that a black hole cannot possess a magnetic field of its own and thus the treatment of Ruffini and Treves is more applicable to the field of a neutron star or a white dwarf.

A black hole in a binary system is known to accrete plasma from either

the companion star or from the interstellar matter and this accretion of charged particles could endow the black hole with a net charge. If a charged black hole is rotating, then there will be an induced dipole magnetic field. Further, these charged particles when they are going around in stable orbits around a black hole would give rise to current loops which in turn could produce magnetic fields. Such sources have been well described and discussed by many authors [15-18, 28]. On the other hand, in the case of single black holes the intergalactic or interstellar magnetic field which could be treated as uniform would be the superposed field. In case the black hole is rotating, due to inertial frame dragging, the field lines get twisted and this could give rise to certain higher multipoles very near the horizon.

DAMOUR *et al.* [43], HANNI [44] and ZNAJEK [45] have discussed the nature of plasma inflow near about a black hole and have shown the existence of plasma horizon and magnetosphere for a black hole. DAMOUR *et al.* have studied the flow of plasma in regions of magnetic dominance by using the guiding-centre approximation, as seen from the local Lorentz frame. The flow lines thus determined are divided into two classes: those that intersect the horizon and those that do not. If the flow lines intersect the horizon, then the plasma flowing along it either accrete to or get swept away from the black hole, de-

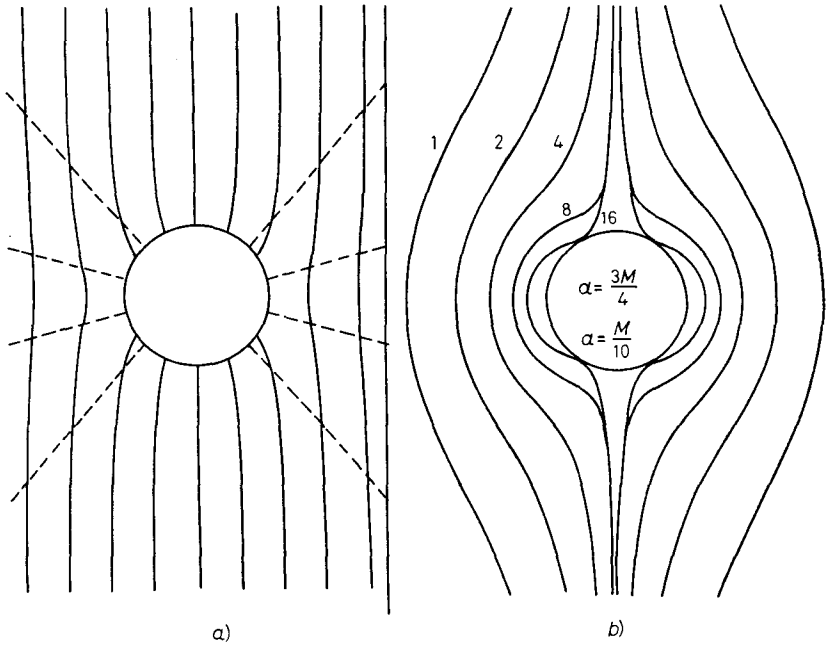

Fig. 24. – *a*) The dashed and the continuous lines represent the electric and magnetic lines of force, *b*) the open curves represent the plasma horizon correponding to asymptotic magnetic-field strengths $B = nQ/m^2$. The circle represents the event horizon of a Kerr-Newmann black hole with its magnetic-dipole moment parallel to asymptotically uniform magnetic lines of force [44].

pending on its charge. Whereas, in the case when the flow lines do not intersect the horizon, the plasma oscillates between two mirror points similar to what has been shown in fig. 23 (ref. [21]) and a magnetosphere can form in this region. The flow line that divides these two classes may have a cusp, unless the electric field is everywhere less than the magnetic field. The surface of revolution generated by this line defines the boundary for the magnetosphere. Figures 24 and 25 show the structure of electric and magnetic lines of force, as well as plasma horizons for the case of a Kerr-Newmann black hole embedded in an asymptotically uniform magnetic field with the dipole moment of the black hole parallel and antiparallel to the external magnetic field. The plasma horizon is defined by

$$F_{\alpha\beta}\eta^{\beta}F^{\alpha\gamma}u_{\gamma}=0\,,\qquad V_{\alpha}V^{\alpha}=0\qquad\text{and}\qquad V^{\alpha}=F^{\beta\alpha}F_{\beta\gamma}\eta^{\gamma}\,, \tag{7.2}$$

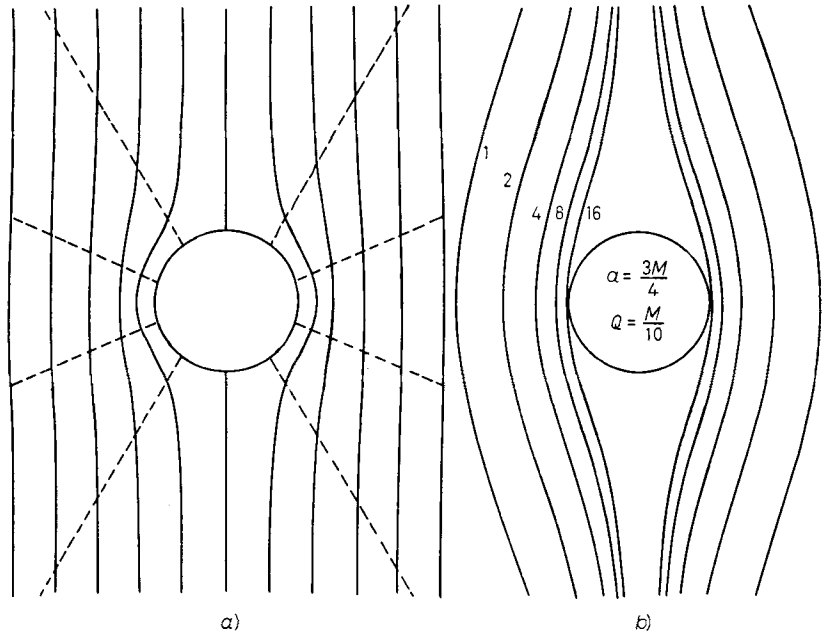

Fig. 25. – Same as fig. 24 but with dipole moment antiparallel to the external magnetic field [44].

wherein u_{γ} is the timelike four-velocity of the test charge and η^{β} is the four-velocity of an observer at rest in the local inertial frame $e^{\hat{}}_{\hat{j}}$ defined by (5.34). As DAMOUR *et al.* point out, in the case when the magnetic moment of the black hole is aligned with the external field the magnetic field in the equatorial plane is weaker and thus the support for a charged particle would be reduced. This would make the plasma horizon as well as cusped flow lines stay farther away from the black hole than in the case when the magnetic moment and the ex-

ternal field are antiparallel. If there is no external field, the flow lines are radial, as the induced magnetic field of an isolated black hole cannot support a magnetosphere against its own electric field. As HANNI has shown, this would mean $V_\alpha V^\alpha < 0$ and thus there is no plasma horizon for an isolated black hole.

Apparently, when the possibility of strong electromagnetic fields around an accreting black hole was first proposed [12] by considering the dominance of the electric field and not taking into account the possible existence of the external magnetic fields, it was thought that the selective accretion of oppositely charged particles would neutralize the charge of the black hole on a short time scale. But subsequent analysis of Damour *et al.*, as mentioned above, has shown the possibility of balancing the electric field of a charged black hole by asymptotically uniform weak magnetic fields, and thus demonstrate the possibility of trapping charged particles in the magnetosphere of a black hole.

Before concluding, it is perhaps useful to make some comments for astrophysical situations as to when a single-particle approach as reviewed above is reasonable. In the general treatment of a plasma in nonrelativistic physics one uses normally a kinetic approach or a fluid (MHD) approach depending upon the scale lengths and densities involved. But, if one considers a relativistic framework, the only kinetic theory that one knows of is the special-relativistic kinetic theory as developed by ISRAEL, ANDERSON, STEWART and EHLERS [46]. Though there are some attempts to work out a generally covariant kinetic theory, this has not been formulated completely as yet. Thus, while treating plasma in general relativity, one confines mostly to the relativistic MHD equations.

But either of these two approaches is required only when collective effects of plasma are important. There could be astrophysical situations wherein collective effects may not be that important. The basic feature as is normally used in « flat space » treatments is that the collective effects are unimportant only when the collision frequency of the particles is much less than the gyrofrequency. Using this criterion, one could directly get estimates on the density depending on the magnetic field and the temperature, for which a single-particle approximation is valid. In the case that we are treating here wherein there are two fields, the electromagnetic and the gravitational (gravitation being dominant), there is no straightforward recipe to get estimates on the density. However, in a limited sense, as the effects of the space-time curvature are taken into the structure of electromagnetic fields, one could make a very rough estimate again in terms of the mean free path and the field gradient. As the effects of space-time curvature have been taken into the structure of magnetic field through solving Maxwell's equations on curved space time, we shall consider the restriction as given by taking the mean free path l greater than the effective field variation scale length,

$$l > |B/(\mathrm{d}B/\mathrm{d}r)|\,, \tag{7.3}$$

B being the effective magnetic field. Considering the general expression for the mean free path of charged particles as given by

$$l = 3.2 \cdot 10^6 / Z^2 n \ln \Lambda , \tag{7.4}$$

wherein $\Lambda = 1.3 \cdot 10^4 n^{-\frac{1}{2}}$ and $n = N/T^2$, N being the particle density and T the plasma temperature, from (7.3) and (7.4) we get

$$n \ln \Lambda < \frac{3.2 \cdot 10^6}{Z^2} \left| \frac{1}{B} \frac{dB}{dr} \right| . \tag{7.5}$$

As an example, if we consider the dipole magnetic field on a Schwarzschild geometry (sect. **5**) with

$$B = \frac{3\mu}{4m^2} \left[1 + \left(1 - \frac{2m}{r}\right)^{-1} + \frac{r}{m} \ln \left(1 - \frac{2m}{r}\right) \right] \left(1 - \frac{2m}{r}\right)^{\frac{1}{2}} ,$$

we get the condition for singly charged particles

$$n \ln \Lambda < \frac{6.4 \cdot 10^6}{r} \left| \left(1 - \frac{m}{r}\right) \left(1 - \frac{2m}{r}\right)^{-1} \frac{A - m/r}{A + m/r} \right| , \tag{7.6}$$

wherein

$$A = 1 + \frac{r}{m} \left(1 - \frac{2m}{r}\right) \ln \left(1 - \frac{2m}{r}\right) ,$$

which for a $1 M_0$ black hole at $r = 3m$ gives the condition $n \ln \Lambda < 52.345$ or $9.5n - (n/2) \ln n < 52.345$, *i.e.* $n \leqslant 5.5$. This in turn gives the condition on particle density as

$$N < 5.5 T^2 . \tag{7.7}$$

This condition looks very reasonable, implying that the density may be higher if the plasma is sufficiently hot, as then the higher thermal velocity will keep the particles quite apart, reducing the interactions between one another. From (7.6) it is obvious that the density has to decrease for a fixed mass as one moves away from the black hole, as also at a given point for the increase of mass of the black hole. The above estimate is a very rough estimate, as the validity of the expression used for « mean free path » may not be rigorous for the case of curved geometry. In any case, if the particle density is greater than few times the square of the plasma temperature, then the single-particle approach treated in the above review will not be sufficient to describe the physical situation.

In conclusion I would like to point out that the study of the charged-parti-

cle motion in electromagnetic fields superposed on black-hole space-times is important from the point of view of accretion as well as radiation emission from high-energy sources. As such, no rigorous treatment exists for the study of particle motion with the radiation reaction being included. The main difficulty in considering such a system is that no Lagrangian formulation has yet been possible for considering motion with radiation. This problem in our opinion is important and needs a detailed consideration.

* * *

It is a pleasure to thank B. BERTOTTI, R. BREUER, B. CARTER, D. K. CHAKRABORTY, J. EHLERS, R. HANNI, W. KUNDT, J. NITSCH, H. RUMPF, J. SHAHAM, E. P. J. VAN DEN HEUVEL, R. K. VARMA, C. V. VISHVESHWARA, M. WALKER, D. WILKINS and R. ZNAJEK with whom I had useful conversations on various aspects of topics covered in the review. In particular I wish to acknowledge the valuable collaboration I have had with D. K. CHAKRABORTY, R. K. VARMA and C. V. VISHVESHWARA concerning the study of charged-particle trajectories. I thank the referee for some useful suggestions.

Note added in proofs.

My attention was recently drawn to the fact that eq. (4.5) has been earlier derived by TOD, DE FELICE and CALVANI (*Nuovo Cimento B*, **34**, 365 (1976)) in the pole-dipole approximation, who have also for the first time found the existence of superluminal velocities for the baricentre. Further EHLERS and RUDOLF (*Gen. Rel. Grav.*, **8**, 197 (1977)) have obtained the same equation (4.5) in general.

The value of r as obtained in eq. (3.15) for the last unstable circular orbit is in fact the same as that for the innermost unstable circular photon orbit in the equatorial plane of the RN metric and thus it is not surprising that it holds independently of particle charge.

REFERENCES

[1] S. WEINBERG: *Gravitation and Cosmology* (New York, N. Y., 1972); YA. B. ZEL'DOVICH and I. M. NOVIKOV: *Relativistic Astrophysics.* - Vol. 1: *Stars and Relativity* (Chicago, Ill., 1972); M. REES, R. RUFFINI and J. A. WHEELER: *Black Holes, Gravitational Waves and Cosmology* (New York, N. Y., 1976); R. GIACCONI and R. RUFFINI, Editors: *Proc. S.I.F.*, Course LXV (Amsterdam, 1978).

[2] R. A. BREUER: *Gravitational perturbation theory and synchrotron radiation*, in *Lecture Notes in Physics*, Vol. **44** (Berlin, 1975); K. M. V. APPA RAO and S. M. CHITRE: *Space Sci. Rev.*, **19**, 281 (1976); E. P. J. VAN DEN HEUVEL: *Proc. S.I.F.*, Course LXV (Amsterdam, 1978), p. 828; D. L. JAUNCY, Editor: *Radio Astronomy and Cosmology, IAU Symposium* 74 (1977); G. H. RIEKE and M. J. LEBOFSKY: *Infra-red emission of extragalactic sources*, to be published (1979).

[3] P. GOLDREICH and W. H. JULIAN: *Astrophys. J.*, **157**, 869 (1969); L. MESTEL: *Nature (London) Phys. Sci.*, **233**, 149 (1971); N. J. HOLLOWAY: *Nature (London) Phys. Sci.*, **246**, 6 (1973); M. A. RUDERMAN and P. G. SUTHERLAND: *Astrophys. J.*, **196**, 51 (1975); M. M. BASKO and R. A. SUNYAEV: *Mon. Not. R. Astron. Soc.*, **175**, 395 (1976).

[4] K. ELSASSER and J. KIRK: *Astron. Astrophys.*, **52**, 449 (1976); V. G. ENDEAN: *Mon Not. R. Astron. Soc.*, **174**, 125 (1976); E. A. JACKSON: *Astrophys. J.*, **206**, 831 (1977); F. C. MICHEL: *Astrophys. J.*, **213**, 836 (1977); **214**, 261 (1977); S. ICHIMARU: *Astrophys. J.*, **214**, 840 (1977); A. F. CHENG and M. A. RUDERMAN: *Astrophys. J.*, **216**, 865 (1977).

[5] S. HAWKING and G. F. R. ELLIS: *Large Scale Structure of Space-Time* (Cambridge, 1972).

[6] F. DE FELICE: *Nuovo Cimento B*, **57**, 351 (1968); D. WILKINS: *Phys. Rev. D*, **5**, 814 (1972); also in *Black Holes, Les Houches Lectures, 1972*, edited by B. DEWITT and C. DEWITT (New York, N. Y., 1972), p. 57; J. STEWART and M. WALKER: *Black Holes, The Outside Story, Springer-Tracts* 69, *Astrophysics* (1973).

[7] W. KINNERSLEY: *J. Math. Phys.* (*N. Y.*), **18**, 1529 (1977); W. KINNERSLEY and D. M. CHITRE: *J. Math. Phys.* (*N. Y.*), **18**, 1538 (1977).

[8] D. M. CHITRE: *Gravitation, quanta and the Universe*, in *Proceedings of Einstein Centenary Symposium, 1979*, edited by A. R. PRASANNA, J. V. NARLIKAR and C. V. VISHVESHWARA (New York, N. Y., 1980).

[9] J. L. SAFKO and L. WITTEN: *J. Math. Phys.* (*N. Y.*), **12**, 251 (1971); R. G. MCLENAGHAN and N. TARIQ: *J. Math. Phys.* (*N. Y.*), **16**, 2305 (1975); W. B. BONNOR: *J. Phys. A*, **12**, 853 (1979).

[10] E. T. NEWMAN, E. COUCH, R. CHINNAPARED, H. EXTON, A. PRAKASH and R. TORRENCE: *J. Math. Phys.* (*N. Y.*), **6**, 918 (1965); C. W. MISNER, K. S. THORNE and J. A. WHEELER: *Gravitation* (San Francisco, Cal., 1972).

[11] B. CARTER: in *Black Holes, Les Houches Lectures, 1972*, edited by B. DEWITT and C. DEWITT (New York, N. Y., 1972), p. 57.

[12] R. RUFFINI: in *Black Holes, Les Houches Lectures, 1972*, edited by B. DEWITT and C. DEWITT (New York, N. Y., 1972), p. 451.

[13] R. HOJMAN and S. HOJMAN: *Phys. Rev. D*, **15**, 2724 (1971).

[14] V. L. GINZBURG and I. M. OZERNOI: *Sov. Phys. JETP*, **20**, 689 (1965).

[15] J. A. PETTERSON: *Phys. Rev. D*, **10**, 3166 (1974).

[16] J. BICAK and L. DVORAK: *Czech. J. Phys. B*, **27**, 127 (1977).

[17] D. M. CHITRE and C. V. VISHVESHWARA: *Phys. Rev. D*, **12**, 1538 (1975).

[18] J. A. PETTERSON: *Phys. Rev. D*, **12**, 2218 (1975).

[19] A. R. KING, J. P. LASOTA and W. KUNDT: *Phys. Rev. D*, **12**, 3037 (1975).

[20] R. M. WALD: *Phys. Rev. D*, **10**, 1680 (1974).

[21] A. R. PRASANNA and R. K. VARMA: *Pramana*, **8**, 229 (1977).

[22] A. R. PRASANNA and C. V. VISHVESHWARA: *Pramana*, **11**, 359 (1978).

[23] A. R. PRASANNA and D. K. CHAKRABORTY: *Pramana*, **14**, 113 (1980).

[24] G. DENARDO and R. RUFFINI: *Phys. Lett. B*, **45**, 259 (1973).

[25] D. CHRISTODOULOU and R. RUFFINI: *Phys. Rev. D*, **4**, 3552 (1971).

[26] R. RUFFINI and F. ZERILLI: in *Black Holes, Les Houches Lectures, 1972*, edited by B. DEWITT and C. DEWITT (New York, N. Y., 1972), p. 75.

[27] A. ARMENTI: *Nuovo Cimento*, **25**, 442 (1975).

[28] R. RUFFINI: *Proc. S.I.F.*, Course LXV, edited by R. GIACCONI and R. RUFFINI (Amsterdam, 1978), p. 287.

[29] M. MATHISON: *Acta Phys. Pol.*, **6**, 163 (1937),

[30] A. PAPAPETROU: *Proc. R. Soc. London Ser. A*, **209**, 248 (1951).

[31] A. R. PRASANNA and N. KUMAR: *Prog. Theor. Phys.*, **49**, 1553 (1973).

[32] M. A. MELVIN: *Phys. Lett.*, **8**, 65 (1964).
[33] K. P. TOD, F. DE FELICE and R. CALVANI: *Nuovo Cimento B*, **34**, 365 (1976).
[34] E. T. NEWMAN and R. PENROSE: *J. Math. Phys.* (*N. Y.*), **3**, 566 (1962).
[35] S. A. TEUKOLSKY: *Phys. Rev. Lett.*, **29**, 114 (1972); *Astrophys. J.*, **185**, 635 (1973).
[36] S. CHANDRASEKHAR: *Proc. R. Soc. London Ser. A*, **349**, 1 (1976).
[37] F. J. ERNST: *Phys. Rev.*, **168**, 1415 (1968).
[38] F. J. ERNST: *J. Math. Phys.* (*N. Y.*), **17**, 54 (1976).
[39] N. DADHICH, C. HOENSELAERS and C. V. VISHVESHWARA: *J. Phys. A*: *Math., Nucl. Gen.*, **12**, 215 (1979).
[40] G. A. ALEKSEEV: *Sov. Phys. Dokl.*, **210**, 336 (1975).
[41] R. RUFFINI: *Phys. Lett. B*, **41**, 334 (1972).
[42] R. RUFFINI and A. TREVES: *Astrophys. Lett.*, **13**, 109 (1973).
[43] T. DAMOUR, R. S. HANNI, R. RUFFINI and J. R. WILSON: *Phys. Rev. D*, **17**, 1518 (1978).
[44] R. S. HANNI: *Proceedings of the I Marcel Grossmann Meeting on General Relativity* (1977), p. 429.
[45] R. ZNAJEK: *Nature* (*London*), **262**, 270 (1976); also Ph. D. Thesis, University of Cambridge (1976).
[46] W. ISRAEL: *J. Math. Phys.* (*N. Y.*), **4**, 1163 (1963); J. L. ANDERSON: *Proceedings of the Mid West Conference on Relativity*, edited by M. CARMELI *et al.* (1970); J. EHLERS: *Proc. S.I.F.*, Course LVII (Amsterdam, 1971); J. STEWART: *Non-equilibrium relativistic kinetic theory*, in *Springer Lecture Notes in Physics*, Vol. **10** (1971).